IMPROVING OSSEOINTEGRATION OF PEEK THROUGH SURFACE TEXTURES

by

Renn Patrick Scott

A thesis submitted in partial fulfillment
of the requirements for the degree

of

Master of Science

in

Mechanical Engineering

MONTANA STATE UNIVERSITY
Bozeman, Montana

August 2019

©COPYRIGHT

by

Renn Patrick Scott

2019

All Rights Reserved

ACKNOWLEDGEMENTS

I would first like acknowledge, Dr. Cecily Ryan of the Ryan Lab at Montana State University my advisor and coauthor for the guidance and expertise required to complete this project.

I would also like to acknowledge Dr. Ron June and Dr. Garth James my graduate committee members for their lab space and guidance for all cellular and statistical matters, Dr. Stephan Warnat and Matthew McGlennen for guiding and assisting in the photolithography process required to create the aluminum molds, and Danah Ashour of the June lab for guiding and managing cell plating, fixation and care.

I would next like to acknowledge Dr Heidi Smith, the Center for Biofilm Engineering for their standing confocal microscope and the training to use it, the MSU Imaging and Chemical Analysis Laboratory for the scanning electron microscope and all the training and sample prep to use it, the Dr Stephen Sofie lab and the Composite Materials Lab for the use of their hot presses.

Finally I would like to acknowledge the Thorson Excellence in Engineering Research Grants Program for funding this project.

TABLE OF CONTENTS

1. INTRODUCTION 1

Background 2
Bone 2
PEEK 3
Research Objectives 5

2. MATERIALS AND METHODS 7

Materials 7
PEEK 7
Aluminum Molds 7
Pre-osteoblast cell line 7
Cell Processing Materials 7
Methods 8
Mask Design 8
Al 6061 Mold 9
Hot Embossing 10
Storage and Cultivation of Pre-Osteoblast Cells 12
SEM 13
Confocal Microscopy 14
Confocal Data Analysis 15

3. RESULTS AND DISCUSSION 17

Hot Embossing 17
Results of MC3T3 Growth 18
Challenges with the $10\mu m$ Samples 18
Live/Dead Counts 19
Cell Volume 27
Cell Distance to Feature 31
Discussion 33

4. CONCLUSION 38

REFERENCES CITED 41

APPENDICES 44

APPENDIX A : Surface Textures 45
APPENDIX B : Cell Mask for Photolithography 78

TABLE OF CONTENTS – CONTINUED

APPENDIX C : Results of Generalized Linear Model 80
APPENDIX D : Piranha Etch Experiments 85
Methods 86
Results 86

LIST OF TABLES

Table Page

3.1 Average Cell Counts 24

3.2 Average Cell Growth 29

3.3 Average Cell Distance 32

3.4 Average Cell Growth with Respect to Shape 36

A.1 Surface Texture Types as seen under SEM on Al Mold 46

LIST OF FIGURES

Figure Page

2.1 Heated Press Used for Hot Embossing 12

3.1 Aluminum Surface after 20 minutes of Etching 20

3.2 $10\mu m$ Single Spaced Circular Hole Displaying Manufacture Errors 21

3.3 $10\times5\mu m$ Cell Growth on Textured vs Un-textured control on $10\times5\mu m$ 22

3.4 $10\times10\mu m$ Cell Growth on Textured vs Un-textured control 22

3.5 A Comparison of Cell Counts Averaged Over Feature Size and Depth and Feature Type 23

3.6 Cell Count Data When Analyzed is Isolated by Feature Size 23

3.7 Cell Count Data When Analyzed is Isolated by Feature Shape 24

3.8 Cell Count Data When Analyzed is Isolated by Feature spacing 24

3.9 Cell Count Data When Analyzed is Isolated by Feature Concavity/Convexity 25

3.10 Cell Volume/Feature Surface Area for each Feature 28

3.11 Cell Volume/Feature Surface Area for each Feature 28

3.12 Average Cell Distance from Feature 31

B.1 Total Cell Mask 79

D.1 Resultant Surface Textures on PEEK from Piranha Etch. Mag×1000 87

D.2 Resultant Surface Textures on PEEK from Piranha Etch. Mag×20,000 87

D.3 Comparison of Cells on Etched and Control PEEK Disks 88

NOMENCLATURE

PEEK	Polyetheretherketone
Ti	Titanium
Al	Aluminium
MCT3T − E1	Pre-osteoblast cell line

ABSTRACT

PEEK (Polyetheretherketone) is one of the most promising alternatives to titanium in cortical bone implants due to being biologically inert and having an elastic modulus similar to that of bone. It also has favorable reactions conducive to common medical imaging methods such as X-ray and magnetic resonance imaging (MRI) as compared to commonly used metals such as titanium and stainless steel. However PEEK is not inherently osseoconductive, leading to longer healing times and a greater chance of infection. Many different methods exist for improving osteoblast growth, such as the addition of bio-active materials like hydroxyapatite. Manipulating the surface texture of PEEK could provide better environments for cells to attach and can be used as another layer with other techniques, making the tissue interface more robust. The main objective of this project is to observe cell adhesion to a textured surface to identify cell preference for surface geometry as a first step to improve full integration of non-resorbable implants into bone tissue. The methods explored were also chosen for their repeatability, reliability and lack of chemical modification compared to other successful surface modulation techniques. The surface textures were embossed into PEEK using micro-etched aluminum molds. Textures vary in their shape, spacing, size, depth and surface convexity/concavity. The cell adhesion was recorded through fluorescent confocal microscopy and the cell-substrate interaction was observed under electron microscopy. The results were that $25\mu m$ and $10\mu m$ features discouraged cell adhesion while $325\mu m$ and $120\mu m$ features encouraged cell adhesion with pillars performing better than holes. The best feature was the $325\times40\mu m$ square pillars. With a cell volume to surface area ratio of 5.13, a live cell count of 276.5, a dead cell count of 9.00, and a non-dimensional distance to feature of 0.67

1

INTRODUCTION

Polymers are a key material in nearly all medical procedures, from bone and tissue grafts, to prosthesis, to controlled release vehicles for medicines [13, 17]. Polymer manufacture allows for the construction of devices with a wide range of properties that make them suitable for use in the human body such as hydrophilicity, modulus of elasticity and cytotoxicity. This project focuses on polyetheretherketone (PEEK) due to its properties making it to be a promising alternatives to titanium (Ti). PEEK is biologically inert and has an elastic modulus similar to that of bone [8]. It also has favorable reactions to common medical imaging methods such as x-ray and MRI as compared to commonly used metals such as Tiand Stainless Steel. Many different methods exist for improving osteoblast growth, such as the addition of bioactive materials like hydroxyapatite [18], or using ion beam sputtering to modify the surface roughness or chemical properties of the PEEK [1, 7]. Most of these methods are either chemical in nature or affect surface texture at the nanometer level. Micrometer scaled patterns have been shown to have an effect on cell behavior as well [3]. The goal of this project is to identify the effect of different surface texture properties for dimensions from $10\mu m$ to $325\mu m$ in PEEK on the initial adhesion of osteoblast cells. This size range means that the textures that exhibit the best cell behavior can be used alongside chemical, biological or nano-roughness treatments for a better total solution.

Background

Bone

Bone is a complex composite generated by the body that can be tailored for many different roles and functions. For the most part bone can be separated by two different tissue types, trabecular or cancellous bone and compact, or cortical bone [14]. Trabecular bone is a spongy material filled with blood and marrow that provides some flexibility to bones as well as playing an important role in the metabolic processes of the body. Cortical bone, which makes up a much greater percentage of the bodys bone tissue than trabecular bone, is the hard composite that adds structural support to bone. It is made of organic fibers forming a matrix that is mineralized with a calcium-phosphate mixture [18]. This tissue is also filled with blood vessels giving bone cells access to good nutrient and waste transport, allowing bone to grow and heal. In embryos, osteoblasts differentiate from stem cells and begin the bone making process. Osteoblasts form into larger groups and deposit a collagen matrix before injecting calcium phosphate into the matrix and hardening it. From this point osteoblasts can differentiate into osteoclasts, which dissolve bone, and osteocytes which embed in the bone and maintain it. Healthy human osteoblasts do not usually reproduce through division, making it difficult to study their interactions in vitro. For this reason, MC-3T3 mouse osteoblasts were used. These cells are mouse pre-osteoblast cells that reproduce readily by division and have a preference for osteoblast differentiation. This allows for a cell that is both readily reproduced in lab environments and will easily become osteoblasts and exhibit proper osteoblast behavior on the experimental substrate. Osteoblasts were deemed to be the most important cell to target in this experiment because they create the environment the other cells will live in. In addition, it is believed that faster bone adhesion and

growth will lead to better wound healing after surgery and shorten the window for infection [16]. Osteoblasts are the most common bone cell in this trabecular-like environment of healing bone, as the body tries to create new bone tissue. A surface texture that encourages cells to both attach and behave naturally would be considered the best candidate for further development.

PEEK

PEEK is a polymer valued for its high working temperature and chemical resistance, which makes it a popular polymer in industry and also makes it biocompatible [9, 15]. Biocompatibility is a characteristic that describes how well a material integrates into the body without causing harm to cells or tissue and without disrupting biological processes. Most materials achieve good biocompatibility by using biological materials as a composite, or by undergoing a process that reduces the surface energy of the material, usually demonstrated by an increase in the material's hydrophilicity [1, 2, 10]. PEEK on the other hand is so chemically resistant that it resists the protein adhesion that can lead to body rejection [8]. PEEK is more hydrophobic and rigid when compared to other biomaterials which makes it less popular for blood rich environments, but makes it an excellent choice as a structural polymer in orthopedic, dental and spinal implants [5, 8, 12]. PEEK comes from a family of polymers referred to as PAEKs (polyaryletherketone) which are characterized by repeated phenylene rings connected by ether or ketone. These groups form into chains of repeating patterns with unique building blocks from one type of PAEK to another. PEEK is a repeated pattern of three rings separated by two ether groups and then a ketone group. Like all thermoplastics, the polymer will form long continuous strands, although the large number of benzene rings cause it to be stiffer than other polymers. PEEK will normally form a semi-crystalline material as a solid

with the ratio of crystalline region to amorphous region being manipulated by the cooling rate, with slower rates resulting in greater ratio of crystalline region.

As Stated, PEEK is particularly interesting for spinal and dental applications due to both its resilience and the modular nature of its mechanical properties. It has a modulus of elasticity similar to that of bone, and is known to be biocompatible [15]. In comparison, the material most commonly used now for these applications is titanium (Ti) which exhibits excellent biocompatibility but causes damage to the surrounding bone over time due to the difference in the modulus of elasticity [11]. This damage from Ti implants is the driving force behind the development of PEEK replacements, but without further development of PEEK's biocompatability, the available applications of the polymer will always be less than that of Ti. There are however, many different methods under development for increasing the bioactivity of PEEK [9]. Bioactivity is the ability of the material to interact favorably with biological processes with the intent of increasing biocompatability. One method commonly explored is using a bioactive material as either a surface coating or a composite. In the applications explored here, the most common bioactive material used is hydroxyapatite due to its chemical similarity to bone [18]. The advantage that hydroxyapatite provides PEEK is that it gives osteoblasts a material that they can chemically bond to instead of the inert surface of PEEK. The downside of using hydroxyapatite as a composite, is that PEEK does not bond well and decreases the strength of the material [6]. On the other hand materials like carbon nano-tubes can increase the strength of the material [4]. Another method of increasing the bioactivity of PEEK is to physically etch the surface with ion beams [**?**, 7]. Using oxygen plasma deposits oxygen groups on the surface of the polymer, decreasing surface energy for potential attachment of cells. Inert gas plasma will also decrease the surface energy of PEEK through the nano-texturing of the material. This is usually achieved through

acid etching or similar chemical techniques, however the chemical resistance of PEEK reduces their effectiveness. Pulsed laser etching has also been experimented with in comparison to or in addition to plasma etching, however wet-ability, and by extension bioactivity was not improved over untreated PEEK [1]. Osteoblast behavior has also been shown to be effected by micrometer scale features in a study that examined cell alignment to 30-50μm grooves set 25μm, 50μm, 75μm and 100μm apart [3]. This study indicated that cells at all length scales responded to the grooves by orienting themselves along the grooves as they grew. This effect was strongest in the denser packed grooves.

Research Objectives

The overall goal of the project was to improve the osseoconductivity of PEEK through surface texture manipulation. A manufacturing technique that reliably creates modular and repeatable surface texture needed to be developed. Preliminary studies with acid-etching delivered nano-scale textures but the reaction was difficult to control and the results were inconsistent. Therefore, hot embossing was selected as a repeatable and reliable method of creating surface textures with the ability to vary feature size, shape, and aspect ratio (width:height). Since osteoblasts can range in size from 20μm to 60μm, as seen in other projects [3, 18] and supported by data collected in this project, length scales on the same order as these sizes were designed. Photolithography was chosen as the as the mold manufacture technique to evaluate surface textures with length scales ranging from 10μm to 325μm. With this method, the following parameters affecting cell adhesion and growth could be evaluated: texture size, shape and spacing, aspect ratio, and concavity/convexity. Texture size, shape, and spacing were evaluated by changing between circular and square patterns with single (features separated by the width of the shape) or double

(features separated by twice the width of the shape) spacing with feature sizes ranging from $10\mu m$ to $325\mu m$. With a highly regular etch rate of $1\mu m$/min, the depth of a feature could be designed as well, thus tailoring aspect ratio. Inverting the regions covered by a mask allowed holes or pillars to be etched into the mold. By systematically changing the feature size, shape, spacing, depth and concave/convex nature, surface textures that optimized osteoblast attachment and proliferation could be determined.

MATERIALS AND METHODS

Materials

PEEK

The PEEK used was sourced from McMaster-Carr (Sante Fe, CA), and came in (12.7mm diameter$\times 91.44cm$) rods(8503K222) and ($15.54cm \times 15.54cm \times 76\mu m$) sheets(8504K11). PEEK acid etching was done with piranha solution made from thermoFisher Scientific Sulfuric Acid (H_2SO_4, 96%) (7664-93-9), and Hydrogen Peroxide (H_2O_2,30%) (7722-84-1) via the campus supply store.

Aluminum Molds

The aluminum (Al) used for the molds was an alloy (6061) from McMaster-Carr, and had a mirror finish (5cm $\times$61cm $\times 814\mu m$) sheet (1655T1). The Al etchant was obtained via Montana State University clean room stores and consists of the proprietary chemical, Aluminum Etchant A, from Transene Company, INC.(Danvers, MA). The resist was AZ 1512 HS from MicroChemicals, GmbH (Ulm, Germany).

Pre-osteoblast cell line

The cell line was the American Type Culture Collection, ATCC (Manassas, VA), MC-3T3-E1, subclone 24, mouse pre-osteoblasts cells (ATCC CRL-2595).

Cell Processing Materials

The following materials used in the plating, expansion and imaging of cells were sourced from ThermoFisher Scientific (Lenexa, KS). The media used to grow the cells was the Gibco, MEM α, Nucleosides (12571063) Media. Dulbecco's Phosphate-Buffered Saline (PBS) with no calcium and no magnesium (14190-250), was used to dilute stains and suspend cells during plating operations. Trypsin

Dissociation Reagent (15090046), was used to detach cells from their expansion plates for further expansion or sample plating. All stains used in the microscopy experiments were sourced from Invitrogen, a company under the ThermoFisher umbrella, and included: Calcien AM (100×) (C1430), Propidium Iodide (PI) (10×) (P3566) and Diamidino-Phenylindole (DAPI) (10×) (D1306), Alexa FluorTM 647 Phalloidin 1/200 dilution (A22287), Alexa Fluore 488 anti-Vimentin Antibody 1/100 dilution (677809), Vybrant Dye Cycle Violet Stain 1/100 dilution (V35003), and MitoTrackerTM Red CMXRoss 1/100 dilution (M7512). Cell fixation was achieved with 4% Paraformaldehyde from Elecron Microscopy Sciences (30525-89-4) and 2% Glutaraldehyde from Sigma-Aldritch (St. Louis, MO).

Methods

Mask Design

The mask was designed in L-edit and prepared for printing in Klayout, and was printed on a transparent polymer sheet by CAD/Art Services, Inc. (Bandon, Oregon). The resolution limit of the mask printer was $5\mu m$ which worked well within the dimensions chosen for the mask. The base dimensions of the surface features were chosen based on an assumed cell size range of $20\mu m$ to $60\mu m$ and manufacturing considerations. The intended feature to cell size relationships were developed as follows: half of a small cell at $10\mu m$, the same size as a small cell at $25\mu m$, the same size of large cells at $50\mu m$, twice the size of a large cell at $120\mu m$ and about five times the size of a large cell at $325\mu m$. The effects of sharp angles, and the geometry of walls were to be observed as well, so features were separated into equal numbers of square patterns and circular patterns. Features can either rise from the substrate or dip into it, so patterns were again separated into holes and pillars. It was hypothesized that the distance between features would affect the ability of cells attached at one feature

to network and communicate to those attached at other features. so all feature pattern types were varied between single spaced and double spaced patterns. Single spacing was defined as the distance required to make the area surrounding a feature equal to the area of the feature, while double spacing made this un-featured area twice as large. An exception was made here for the 325um sample as a double spacing was assumed to be too large to make a difference in cell growth. Instead a feature consisting of one 325um circle surrounded by four equidistant 120um circles was used. This would allow the observation of cells on 325um features that can easily network to other features but still be manufactured in the same manner as the other features. This was not repeated for square features as the distance required for these features would have them overlap with other features and control regions. These control regions would be placed at the intersecting corners of four difference textured regions. The final texture characteristic to be varied is the depth of the surface textures although that could not be controlled by mask design but instead by the etch duration of the Al 6061 mold. A reference table of the patterns as they appear on the Al mold can be found in Appendix A.

Al 6061 Mold

The Al molds were created through photolithography micro-machining. In this process the mirror-finished side of the aluminum sheets had the AZ 1512 HS photoresist deposited onto it with a spin-coater. Spin coating relies on using centrifugal force to evenly spread the resist over the sample. Since the samples are square, this caused some concern with the resist being thicker in the corners of the sample but had no noticeable effect in the final product. The mask was then placed over the resist-coated sample and exposed to UV light, weakening the coating not protected by the mask, allowing it to be rinsed off using solvents. This leaves a

photoresist copy of the mask on the Al sample. Once exposed to the etchant, the surface of the aluminum not covered by the resist will start to erode, preserving the pattern from the mask onto the finished mold. The etch exposure time had two important consequences for the project. The first is that, since the Aluminum Etchant A has a linear etch rate of one micrometer per minute, exposure time was the method that controlled feature depth. The second is that since the etchant was isotropic, it eroded the aluminum equally in all directions. This had a strong effect on the geometry of the final features, and required a change in the design of the targeted feature depths. Initial depths were suppose to be 20um and 40um for all features. At these depths, an average sized cell could cover the entirety of a feature wall at 20um but not at 40um. This was achieved for $325\mu m$ and $120\mu m$ features but smaller feature sizes of 50um, 25um and 10um need to be etched at less extreme depths or the features would erode completely, so the depths close to the texture dimension and half of that depth were chosen. The 50um and 25um textures shared one mold and so were etched to a depth of 20um and 10um while the 10um mold were etched to depths of 10um and 5um.

Hot Embossing

Hot Embossing is a manufacture method where a polymer is heated above its glass transition state and then pressed against a mold under high pressure. This is similar to injection molding except the polymer never reaches melt temperature and is in direct contact with the mold instead of entering the from a flow chamber. The $80\mu m$ thick film was cut into squares with a small overhang beyond the outer dimensions of the mold, ensuring full contact with the mold. The mold and the PEEK were held between two pistons within a square die. Heat is applied through both the top and bottom plates of the press, and pressure is applied through a hydraulic hand

pump below the bottom plate. The PEEK was then pressed against the mold at 18kN, 250°C, for 8 minutes. The glass transition temperature of PEEK is 143°C and the melt temperature is 343°C, so 250°C is enough to imprint most patterns into PEEK. The $10\mu m$ features did not imprint well into the PEEK sample. This is mostly because of feature erosion in the Al mold from the etchant. However, better quality PEEK features might have been achieved if the press temperature was higher. The decreased viscosity of PEEK at a higher temperature would have allowed for the material to more fully fill the hole features of the Al mold. Since the maximum temperature of the press was 250°C, the pressure and press time were increased to the before mentioned 18kN and 8min to compensate. The die and piston system underwent thermal expansion, eventually binding the pistons inside the die. This would decrease the feature quality in the sample over time, leaving large un-textured regions, visible under visual observation regardless of feature dimension. The effect of the expansion could be delayed with sufficient silicon based lubrication but did limit effective operation time to 4 hours which was enough to make 24 samples at one sample every 10min. In Figure 2.1 the hot press used for the embossing can be seen. The top and bottom plates were both heated to 250°C. The sleeve with a long die inside was set on the bottom plate. The PEEK and Al mold were set on top of the bottom die, fitted inside the sleeve. The PEEK was cut to be approximately 5mm larger than that of the sleeve interior. When the top, short die is put on top of the polymer and mold to hold them in the sleeve, the excess PEEK comes out of the top around the die forming a "skirt". The bottom plate is lifted using a hydraulic hand pump, applying pressure to the PEEK. The pressure is measured with a pressure gauge in psi, which made conversions for the pressure on PEEK simple due to the area of the mold being one square inch.

embossing.png



Figure 2.1: The the upper and lower steel plates are heated to 250°C +/- 5°C with the top plat more often being 245°C and the bottom plate more often at 255°C. The sleeve held a lower die the held the PEEK and mold approximately 1 cm below the top of the sleeve. The upper die is shorter and presses the PEEK and mold together at 18 kN. The plates, sleeves and dies were all stainless steel and transferred heat rapidly, requiring only three minutes of heating until the sample was up to 250°C. The excess PEEK material can be seen projecting from the sleeve. For the first run the mold was placed below the PEEK. Later runs placed the mold on top of the PEEK so that the samples held media and did not require as much media during cell plating.

Storage and Cultivation of Pre-Osteoblast Cells

The MC3T3 ostebolast cells used in this study came in a cryo-preserved vial from ATCC. In order to be used, the MC3T3 cell vial was thawed and suspended in the Gibco growth media, where it was allowed to attach and expand in a six-well

plate. After 24 hours, the cells were inspected under the 20X phase inverted light microscope. If the cells had formed an 80-90% confluent mono-layer, the cells could be utilized for either further expansion or plated onto PEEK samples. In this case the cells would be unattached from the substrate with the Trypsin enzymes, otherwise healthy cells would be returned to the incubator and checked in another 24 hours while contaminated populations were sterilized and disposed of. If the cells could be used, the spent media was aspirated, and the cells were washed with 1mL 1X PBS twice. Then 1mL of Trypsin dissociation media was added to detach adherent cells under 5 minutes of incubation. Cells were then drawn into a pipette and the single cell suspension was transferred into 15 mL tube. At this point the Trypsin had to be neutralized with 4mL of media, and the cells could then be split and added to either the samples or the expansion well plates. When being expanded, the cells would be reduced by a ratio of 1:6, with the number of cells grown to confluence in one well plate being spread equally to an area equivalent to six-well plate. PEEK samples were sterilized through acetone and ethanol rinses followed by autoclaving. The volume of cell suspended media would be determined through cell counting, with the target number of cells for a PEEK sample being 2×10^5 to 5×10^5 cells. The newly plated samples would be incubated for 72 hours. A sample would typically be fixed or imaged after 78 hours of incubation, but all samples that contributed to the final data were incubated for 72 hours and used within 12 hours after that.

SEM

Scanning Electron Microscopy (SEM) could not be used directly with the samples due to the polymer overcharging and the vacuum damaging or removing cells from the sample. Samples with cells were fixed with a mixture of 4% paraformaldehyde and 2% glutaraldehyde at -20°C. Samples were then fixed with

Osmium tetra-oxide, rinsed in a 0.2M NaCacodylate buffer solution and dehydrated using increasingly strong concentrations of ethanol until the material was rinsed in two successive baths of 100% ethanol. The sample would then be critical point dried in liquid CO2 which removes any latent liquid from the sample whether its ethanol or water based. This protects the detail of microscopic life from the damage these liquids would cause during the evaporation they would undergo once exposed to vacuum. The samples can then be sputter-coated with gold or iridium at 20mA for 60 seconds. PEEK, like most polymers is non-conductive and had to be sputter-coated in order to be viewed under SEM. Images from the SEM could be used for the observing cell morphology and processed in ImageJ software to measure distances and areas. SEM was used to measure average cell size, etched aluminum porosity, acid-etched PEEK feature size and the error between manufactured feature size and designed feature size.

Confocal Microscopy

Cells could be imaged live through many microscope methods but standing confocal microscopy offered two major advantages over other fluorescent microscopes. The complex three dimensional nature of cells growing over the features is best viewed through a confocal microscope that can be finely focused for different z-stacks in the sample. The standing confocal allows for a wide range of focuses within a submerged sample compared to the inverted confocal. This is good for these samples as the mm scale bends that can occur during manufacture can greatly change the substrate height without having any effect on the features on the μm scale. The Leica Confocal system is equipped with computer software that can scan a region of interest over multiple z-stacks and then store the fluorescence data for each channel excitation that can be later rebuilt into three dimensional shapes representing the cell growth. The

two main stains used to measure cell volume were Calcien AM which stained live cell membranes and PI which stains dead nuclei. DAPI can be used to indicate live cell nuclei but the interference from PEEK's auto-fluorescence reacted strongly under UV excitation and masked the nuclei of most cells since they were adhered directly to the polymer. This strong reaction did allow the UV wavelength to be used as a reflection for the surface return feature topography. Fixed cells could also be imaged under upright confocal with fluorescent stains. This allows for the imaging of details within preserved cells. When imaging live cells, the stains and imaging environment will slowly kill the cells. This process takes a long time but fixed cells will maintain cell morphology for weeks or longer if kept cool. The stains used in this application were Alexa 488 for cytoskeletal membranes, Alexa 647 and Vibrant Violet for nucleic proteins and Mitotraker which marks mitochondria in the cells. Overlap between the excitation and emission of different stains and the PEEK material can be accounted for through three ways. Lieca software has precise filters for what wavelengths are recorded for each excitation laser, it can also do post processing for dye separation to further eliminate cross fluorescence. The Imaris post processing software used to process the confocal data could also edit displayed intensity levels for any one data channel.

Confocal Data Analysis

Confocal z-stack scans were compiled in Imaris software and had the background intensity filtered out. Imaris uses metadata and the recorded images to build a three dimensional model of the recorded feature. These models can be isolated by channel, so a model of just the Calcien AM stained Cellular membrane was created. The metadata included magnification data and z-scan height, so Imaris can calculate values with a true scale. The viewed area of each sample was $650\mu m^2$ and the height

would depend on feature size and sample orientation. Using this data the volume of the cell membrane and therefore the total volume of cell growth in the sample can be recorded. This cell volume was compared against the theoretical surface area of the feature that it was grown on to create a ratio of volume to surface area. This allows the comparison between cell growth between the different texture features and also samples that were imaged at an angle due to bends in the material. This did not change the cell volume data relations between different textures for raw volume data and the data divided by surface area. The confocal images were also processed for cell viability. This was measured by compiling the image stacks in ImageJ software, moving through each layer and counting new cells. Z-stacks were kept separate but the different color channels were merged. Cells without visible nuclei and the green Calcein AM stain were counted as live and cells with red nuclei from the PI staining were counted as dead. These cell counts were then compared against each other and against those of other features. Comparing these numbers as ratios of live to dead were not useful due to the much lower cell counts in some features. ImageJ also allowed for the measurement of cells and their location with respect to features. All channels and stacks were merged and the critical dimension of the feature measured. For circles, this was the diameter while for squares it was the length of one side. Another shape 50% larger was drawn onto the image. The number of cells on the feature was counted and compared to cells on the feature. Then the distance from each cell off of the feature to the center of the feature was measured. The average of this distance was divided the distance by the critical dimension of the feature, allowing for comparisons between features of different sizes with different regions of influence.

RESULTS AND DISCUSSION

Hot Embossing

Hot embossing was selected due to its repeatability in creating consistent surface textures without chemical effects. This was determined after a number of inconclusive experiments with growing cells one piranha etched PEEK, the details of which can be found in Appendix D. The isotropic nature of the etch and its effects on the features in the Al mold had very important consequences for the final PEEK sample and cell adhesion. In theory, an isotropic etch will erode in all directions at once, however the actual mechanics of this is through the erosion of small spherical pits in the substrate. These spheres expand until they intersect with other expanding pits and break away larger sections of Al. The average diameter of these pits was measured at $11.75\mu m$ which is larger than the smallest feature dimension at $10\mu m$. The resolution for these shapes was controlled by these small pits. It is analogous to drawing with pixels, the $10\mu m$ feature was drawn with one pixel while the $325\mu m$ feature was drawn with 32 pixels. This loss of resolution led to the loss of some $10\mu m$ features and the reduction of resolution for some $25\mu m$ features. This loss was greatest in the the deeper features, $10\times10\mu m$ and $25\times20\mu m$. The next most important consequence was that there were no right angles for any feature, regardless of size. It was an initial objective to compare cell growth on curved features against angled features to test the hypothesis that cells would avoid attaching to right angles. The loss of the right angle removed some of the significance in having square features as opposed to circular features. There is still value in comparing cells growing against a straight wall as opposed to one curving away as seen from the cell. The combination of angle smoothing and resolution loss was that the top and bottom of features were smooth curves and that the walls were not vertical but had varying slopes depending on the feature depth. The geometry

at the bottom of the PEEK features were mirrors of the geometry at the top of the AL mold. Under etching, this would have been the mirror-finish surface protected by the photoresist. The maximum heat of the press was 250°C and was far less than the PEEK melting temperature of 343°C. Unlike injection molding, hot embossing does not require the material to melt, but the decreased viscosity of a hotter polymer may have resulted in better feature quality, especially in the $10\mu m$ features. The error from the erosion of the $10\mu m$ features during the etching process was great enough that it was impossible to discern if there was error from low temperature during the hot embossing process.

Results of MC3T3 Growth

Challenges with the $10\mu m$ Samples

The 10 μm samples were unable to be compared to the other sized samples due to the erosion of features from the aluminum etch. A test piece of etched aluminum was imaged with the SEM and the pores created by the etch were discovered (Figure 3.1). The average width of these pores was measured at $11.75\mu m$. Features made from these defects imprinting during hot embossing are the same size as the $10\mu m$ features but located randomly throughout all the patterns (Figure 3.2), invalidating $10\mu m$ samples since the metrics that are suppose to be carefully controlled so that different surface textures can be categorically compared are disturbed or destroyed in these samples. Confocal examination of these samples revealed very few cells on textured regions. Due to the similarity between controlled surfaces with features from etching defects and most of the $10\mu m$ features, the designed regions could not be consistently found under confocal. In consequence, a statistically relevant amount of data could not be obtained through confocal measurements to compare cell volume and cell viability with other features. Under SEM imaging the cells could be observed

interacting with the substrate, and cells could be counted but without SEM stains, cells that were alive at fixing can not be discerned from cells that were dead at fixing. Cell volume is also impossible to determine through SEM due to far less precise z-direction focusing compared to confocal imaging and due to fixed cells being opaque to the electron beam and obscuring any cellular morphology below the surface layer. Therefore $10\mu m$ samples could not be compared with other features when determining the optimal feature size.

In Figure 3.3 the effects of the $10\times5\mu m$ single spaced square holes can be compared to the cell growth on the control regions. Many more cells were adhered from the fixation process then was observed under confocal microscopy, but the degradation of the square features can be observed in Figure 3.3a. The Cells clearly overlap and some of the larger cells could be multiply cells that are indistinguishable from each other without fluorescent staining, as can be seen in Figure 3.3b. The $10\mu m$ deep $10\mu m$ samples did not exhibit as pronounced of a difference in cell growth between the control and imprinted region. However the texture imprint in the $10\mu m$ deep samples (figure reference) were degraded and polluted with etch defects that the textured and control regions were too similar for this comparison to be meaningful as can be seen in Figure 3.4. The errors with the manufacture of the $10\mu m$ samples disqualifies it for comparison with other features.

Live/Dead Counts

When comparing averages, larger feature sizes had both higher total cell counts and larger numbers of live cells than smaller features. $325\times40\mu m$ sample had the greatest count of live cells while $25\mu m$ samples had the least. For all features except for $325\mu m$ features the shallower feature had better cell counts than the deeper feature. The mixed circular pillars had the greatest cell growth amongst feature types but this

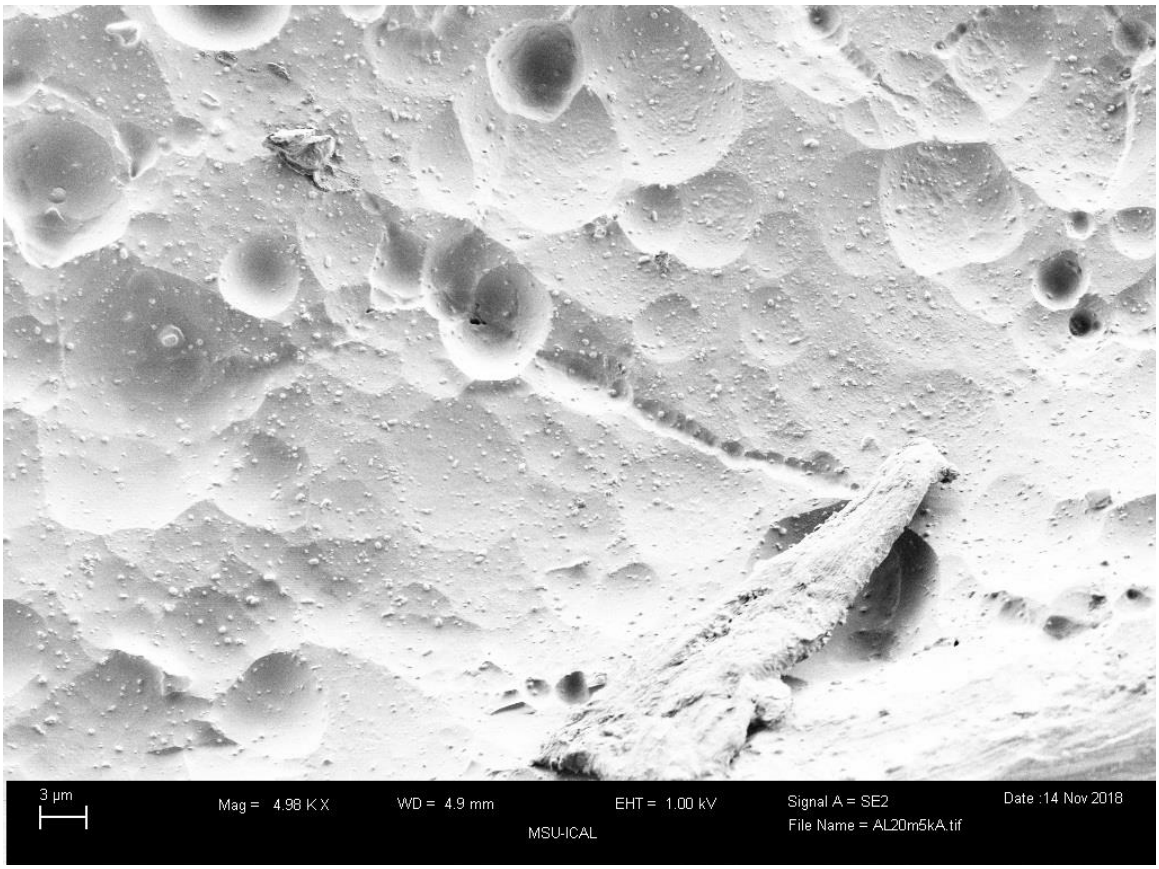


Figure 3.1: Aluminum Etchant A is an isotropic etch, and erodes the Al in all directions simultaneously. In practice this process occurs by the etch forming numerous small spheres that then intersect to separate larger pieces of Al. The average diameter of these spheres was $11.75\mu m$. Visual observations suggest that the depth varies depending on how deep the etch erodes before intersecting another sphere. The linear shape on the bottom of the image is debris that affixed itself before the sputter coating process.

was a feature only present on $325\mu m$ features, the most populous size, which skews the data. For features present in multiple feature sizes, the single spaced square features have the highest live cell counts with single spaced circular pillars having similar cell counts. Double spaced circular pillars are the only pillar that had lower live cell counts on average compared to its hole counterparts. All hole features and double spaced circular pillars had fewer live cells on average than the control regions.

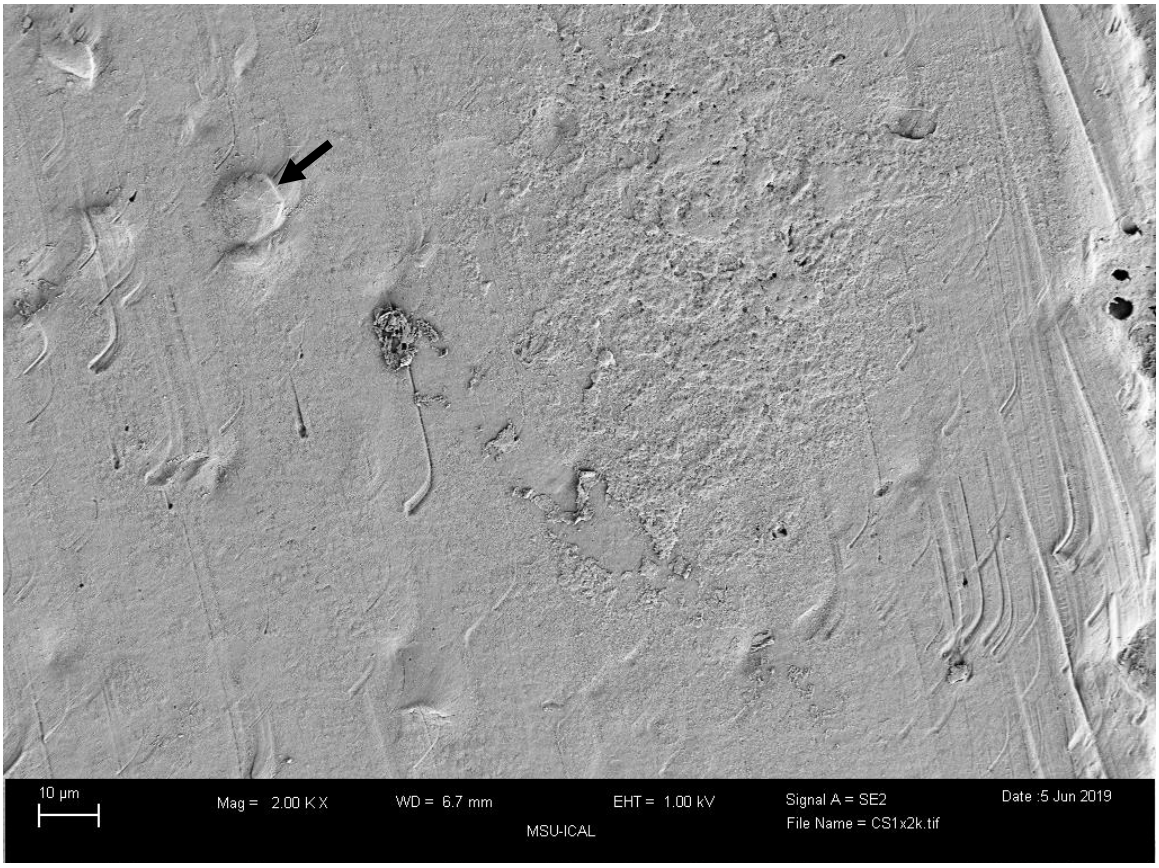
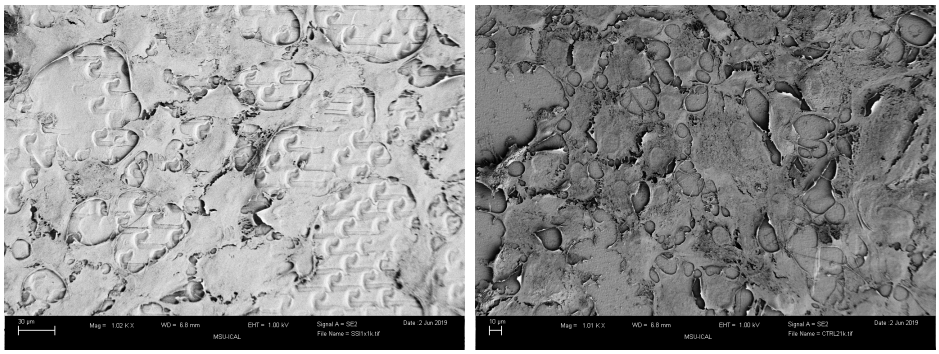


Figure 3.2: The feature labeled with the arrow is a pillar formed from a deeply etched pore. The lines across the surface are where the features should be, but were deformed due to the eroded and missing features on the Al mold. The linear nature of the defects are from removing the sample from the mold.

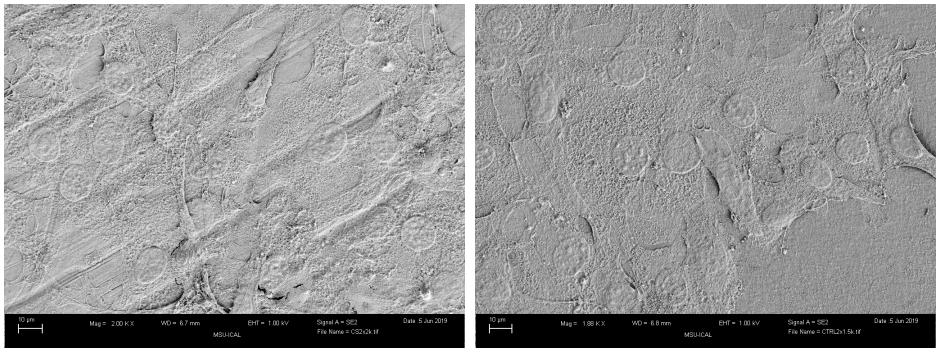
This could be skewed due to the $325\mu m$ features having much higher cell counts in the control regions than other samples. The $120\times20\mu m$ samples had the highest dead cell count on average while $50\times20\mu m$ had the lowest. Single spaced square pillars had the highest dead count cell amongst feature types followed closely by mixed circular pillars. Double spaced square holes have the lowest dead cell count. Using analysis of variance (ANOVA), it was determined that the only result with statistic significance is the size of the feature. Both the $120\mu m$ and $325\mu m$ samples were found to have more live cells than the control samples through Bonferroni's multiple comparisons



(a) Single Spaced Square Holes $10\times5\mu m$

(b) Control Surface on same $10\times5\mu m$ Sample

Figure 3.3: $10\times5\mu m$ Cell Growth on Textured vs Un-textured control on $10\times5\mu m$



(a) Single Spaced Circular Holes $10\times10\mu m$

(b) Control Surface on same $10\times10\mu m$ Sample

Figure 3.4: $10\times10\mu m$ Cell Growth on Textured vs Un-textured control

test. It is important to note that the data was not perfectly normal, and therefore ANOVA analysis should not be considered perfectly accurate. For this reason the rest of the discussion will relate to the comparison of average data across all samples taken within a feature type. This is less useful for concrete conclusions but suggests some interesting data for follow on studies. Review Appendix C for a complete report on the statistic analysis done on cell counting data.

The $325\mu m$ samples were unique from other features in that it did not have

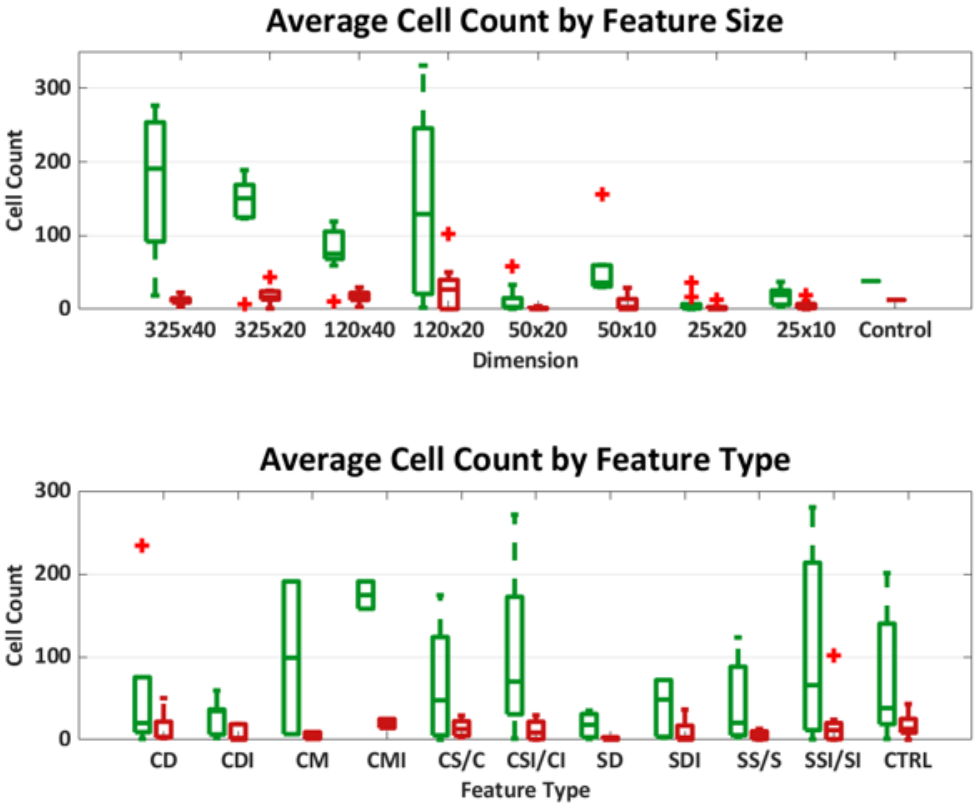
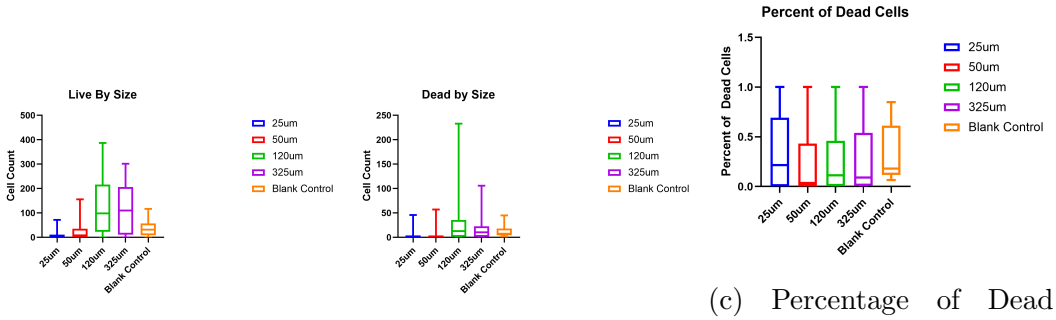


Figure 3.5: A Comparison of Cell Counts Averaged Over Feature Size and Depth and Feature Type

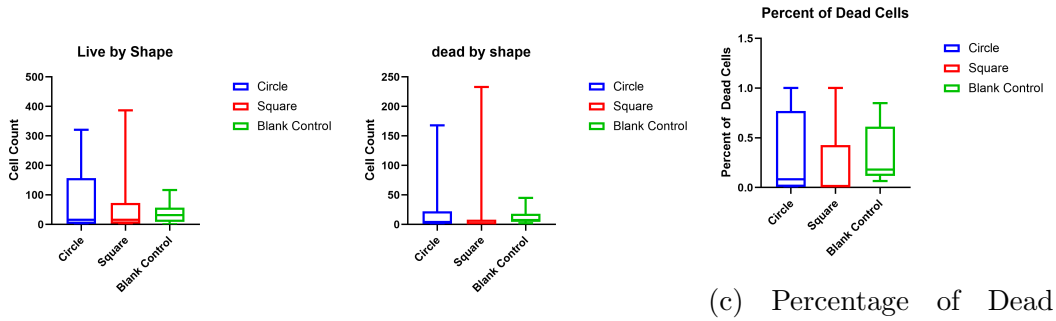


(a) Live Cell Counts (b) Dead Cell Counts (c) Percentage of Dead Cells to Total Cells

Figure 3.6: Cell Count Data When Analyzed is Isolated by Feature Size

Table 3.1: Average Cell Counts

	325X40		325X20		120x40		120x20		50X20		50x10		25X20		25x10		CTRL	
	Live	Dead	Live	Dead	Live	Dead	Live	Dead	Live	Dead	Live	Dead	Live	Dead	Live	Dead	Live	Dead
CD					75.33	21.67	234.29	50.14	9.00	1.75	30.00	2.50	1.00	3.33	10.00	3.33		
CDI					59.33	18.67	2.00	0.00	33.00	2.00	36.00	0.00	36.50	2.00	6.33	19.00		
CM	191.00	9.00	6.67	1.00														
CMI	191.00	14.00	158.00	25.00														
CS/C	58.75	11.75	128.71	21.71	119.00	14.00	174.22	22.89	4.50	4.00	36.50	29.00	0.00	2.67	5.00	5.75		
CSI/CI	271.67	15.00	188.83	16.67	71.25	29.50	69.00	26.67	58.33	0.00	156.00	0.00	1.33	1.33	3.00	2.00		
SD					11.00	3.00	25.00	0.00	3.00	0.33	31.00	3.00	1.00	0.00	35.00	0.00		
SDI					72.00	17.00	331.00	36.33	2.33	0.00	60.00	4.00	3.50	0.00	37.00	1.33		
SS/S	18.50	3.50	123.33	12.67	116.67	7.67	8.00	0.33	2.67	1.00	59.40	13.00	2.67	0.00	22.20	5.25		
SSI/SI	276.50	9.00	150.67	14.00	101.67	24.00	280.33	101.67	0.50	0.50	30.00	16.00	1.50	0.00	21.67	1.00		
CTRL	201.00	22.50	172.50	43.00	83.50	20.50	129.20	32.60	1.00	0.67	36.00	0.00	17.00	13.00	19.33	11.00	38.10	12.60



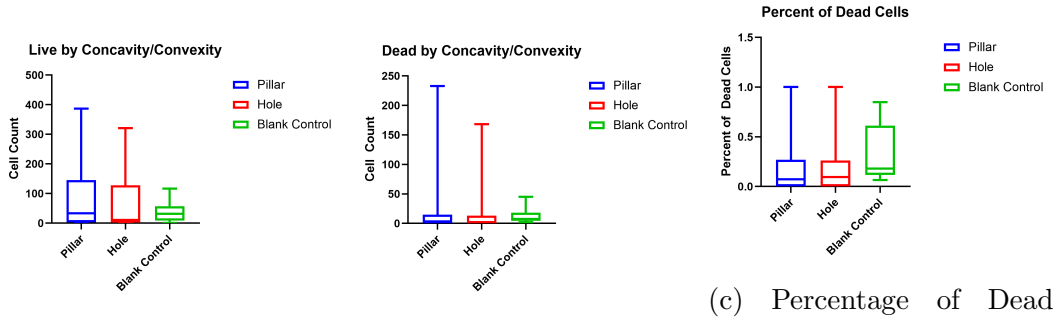
(a) Live Cell Counts (b) Dead Cell Counts (c) Percentage of Dead Cells to Total Cells

Figure 3.7: Cell Count Data When Analyzed is Isolated by Feature Shape



(a) Live Cell Counts (b) Dead Cell Counts (c) Percentage of Dead Cells to Total Cells

Figure 3.8: Cell Count Data When Analyzed is Isolated by Feature spacing



(a) Live Cell Counts (b) Dead Cell Counts (c) Percentage of Dead Cells to Total Cells

Figure 3.9: Cell Count Data When Analyzed is Isolated by Feature Concavity/Convexity

double spaced features, all features were spaced so that the area around the feature was the same as the area within a feature's cross sectional area. They instead featured a mixed circular pattern where $120\mu m$ circles were located halfway between $325\mu m$ circles. The greatest number of live cells were in the $325\times40\mu m$ single spaced square pillars at 276.50 live cells with Circular pillars having a similar number of live cells at 271.67 live cells. The least populated features were the single spaced circular holes at 18.50 cells. The best performing surface feature for $325\times20\mu m$ was the circular pillars at 188.83 cells with the worst feature being the mixed circular holes at 6.67 cells. It is important to note that the control surfaces for both $325\mu m$ samples had much larger cell counts then the control region for any other sample size or the un-patterned control sample.

In the $120\times40\mu m$ samples, the samples also had the added complexity of varying the spacing of features, between single and double spaced features. The highest counts were amongst the single spaced circular holes, single spaced square holes and single spaced square pillars with a respective 119.00, 116.67 and 101.67 average live cells. The double spaced features had a much closer range of live and dead cells. The double spaced circular holes had a live/dead average cell count of 75.33/21.67 while

the double spaced circular pillars had an average count of 58.33/18.67. These values indicate a much higher percentage of dead cells to live cells in these samples compared to the 325μm samples, approximately 20% of the total cells counted each. the double spaced squares show similar behavior with the holes having a ratio of live/dead cells of 11.00/3.00 and pillars having a ratio of 72.00/17.00, with dead cells accounting for approximately 20% of the cells counted.These trends are similar to those of the 325μm features except the larger amount of dead cells and the reduced viability of the double spaced features. For the shallower, 120x20μm features, none of the features seemed to match any of the established trends. The double spaced circular holes had a cell count of 234.29/50.14 while the pillars had effectively no cells at only two average live cells per sample. the single spaced circles also had more cells on the hole version than the pillar with 119 and 71.25 average live cells respectively, but for both single and double spaced square features, the pillared version out-performed the holes by a large margin.

As the feature size decreases, the cell viability drops off quite heavily. The 50×20μm sample exhibited very little cell growth on the square features . The circular features had better cell growth in the pillar than the hole feature with the double spaced features having a hole and pillar cell count of 9 live cells to 33 live cells on average. Single spaced circular holes had 4.5 live cells on average while the pillars had 58.33 live cells on average. The only feature with a number of dead cells relevant to the live cell count was the single spaced circular holes which had a live/dead count of 4/4.5. The 50×10μm features had a greater cell growth than that of the the 50×20μm features but mostly less than that of the larger features. Most features, hole or pillar exhibited approximately 30 live cells per feature. the exceptions include the single spaced circular pillars had a live dead cell count of 156/0 cells on average. The double spaced square pillars and the single spaced square holes also featured approximately

60 live cells on average as opposed to 30. The single spaced square holes and pillars and the single spaced circular holes also had a greater number of dead cells on average than the other features. The single spaced circular holes had 29 dead cells on average, just shy of 50% of the total number of cells counted.

The $25\times20\mu m$ samples had almost no cells to count with total averages of 7.16 live cells for $20\mu m$ deep features and 17.73 live cells for $10\mu m$ deep features. The doubles spaced circular pillar exhibited the best average live cell count at 36.5 live cells compared to only an average of 2 dead cells per sample. This feature also exhibits better cell growth on its control samples than that of most of the textured regions, although there were also a number of dead cells here, with a live/dead count of 17/13. Once again, the shallow features of $25\times10\mu m$ grew cells better than those at the $20\mu m$ depth. the square features had greater cell counts than the circular regions and had a better live/dead ratio. The double spaced square holes had 35/0, the double spaced square pillars had 37/1.33. The single spaced square holes had 22.2/5.25 and the single spaced square pillar had 21.67/1.00. The circular regions did not have any region with greater than 10 live cells per sample on average, and usually featured an equal number of dead cells. The double spaced circular pillars had the most cells fro any circular feature at on this scale with a live/dead ratio of 6.33/19.00.

Cell Volume

Samples with out cell growth were discarded when calculating the ratio of cell volume to theoretical surface area of a sample. This ratio is used to represent a measure of cell growth. The statistical viability of these values was not ascertained due to the way they were measured and calculated so the following comparisons are made for the averages. The features with the largest volume of cells was the $325\mu m$

Cell VolumeEoM.png

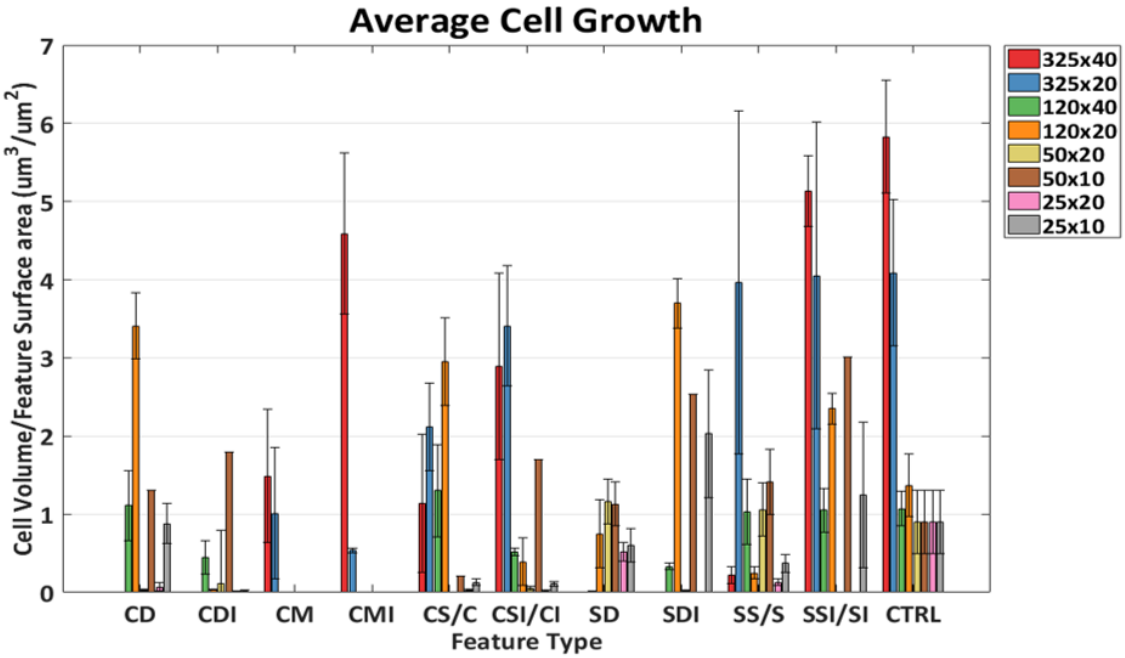


Figure 3.10: Cell Volume/Feature Surface Area for each Feature

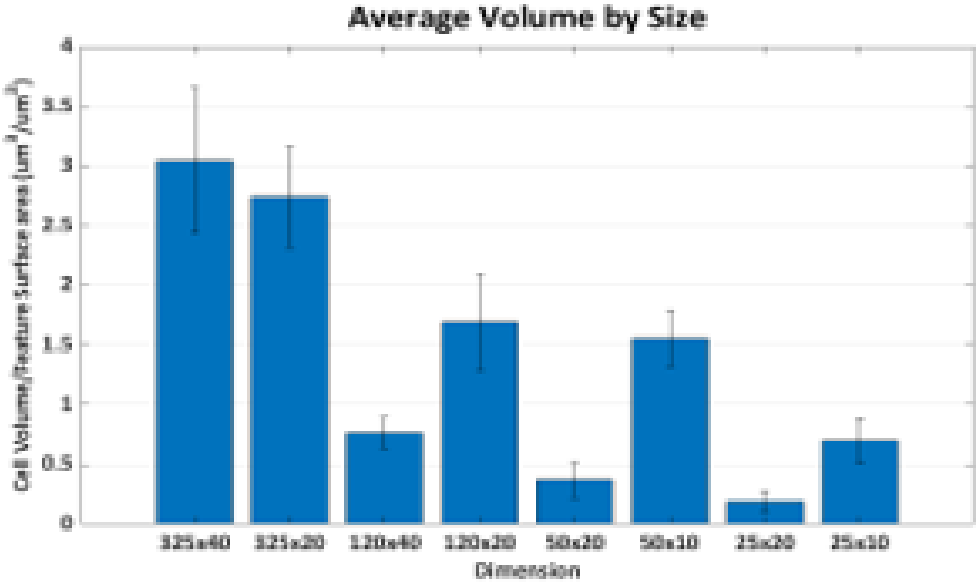


Figure 3.11: Cell Volume/Feature Surface Area for each Feature

Table 3.2: Average Cell Growth

325×40	325×20	120×40	120×20	50×20	50×10	25×20	25×10	
		1.11	3.41	0.03	1.31	0.07	0.87	CD
		0.45	0.04	0.11	1.78	0.02	0.02	CDI
1.48	1.01							CM
4.58	0.53							CMI
1.14	2.12	1.30	2.94	0.01	0.20	0.03	0.12	CS/C
2.89	3.43	0.52	0.39	0.04	1.70	0.01	0.10	CSI/CI
		0.01	0.75	1.16	1.12	0.51	0.59	SD
		0.32	3.70	0.02	2.54	0.01	2.03	SDI
0.22	3.95	1.02	0.25	1.06	1.41	0.12	0.36	SS/S
5.13	4.05	1.05	2.35	0.01	3.01	0.01	1.25	SSI/SI
5.82	4.08	1.07	1.37	0.90	0.90	0.90	0.90	CTRL
3.042489	2.74	0.76	1.69	0.37	1.55	0.18	0.69	Ave Total

features with relatively close volume/surface area ratios of 3.04 for the $40\mu m$ sample and 2.74 for the $20\mu m$ sample. The feature that did the best overall was the control regions of the $325\times40\mu m$ sample with volume/area ratios of $5.83\mu m$. The square pillars had a ratio of 5.13 and the mixed circular pillar region had a ratio of 4.59. These three features had the highest cell growth across all features tested. The worse performing region in the $325\times40\mu m$ sample was the square holes with a ratio of just 0.22. The best performing region of the $325\times20\mu m$ sample was also the control region followed by the square pillar region with ratios of 4.08 and 4.05 respectively. However, in this sample, the square holes also performed well with a ratio of 3.96. The circular regions did poorly compared to the square regions with the hole region having a ratio of 2.12 and the pillar region having a ratio of 3.43. In the $40m$ deep sample, the pillar

region had a ratio of 2.89 while the holes had a ratio of 1.14. The 20μm deep sample on the other hand had a pillar ratio of 3.43 and a hole ratio of 2.12. On this scale, pillars had more cellular growth than holes fro both depths.

In the 120μm the feature with the highest cell growth in the 120×40μm sample was the double spaced circular holes with a ratio of 1.11 followed by the single spaced circular holes at 1.30. The single spaced square pillars and single spaced square holes had very similar ratios at 1.05 and 1.03 respectively. the double spaced square features, the double spaced circular pillars and the single spaced circular pillars all had ratios of less then one. The shallower sample generally had better cell growth in comparison to its deeper counterpart. The greatest cell growth occurred in the double spaced square pillars with a ratio of 3.70. The double spaced circular holes had a volume to surface area ratio of 3.41, the single spaced circular holes had a growth ratio of 2.95 and the single spaced square pillar had a ratio of 2.35. The other non-control surface had a ratio of less then one in this sample.

At the 50μm length scale, cell volume starts to decrease overall. The 50×20μm sample had two regions with a cell volume to surface area greater than one, the double spaced square holes at 1.16 and the the single spaced square holes at 1.06. the 50×10 sample exhibited much greater cell growth with the best region being that of the single spaced square pillars with a ratio of 3.01 followed by the double spaced square pillars at 2.54, the double spaced circular pillars at 1.79, the single spaced circular pillars at 1.70 and finally the single spaced square holes at 1.41. all other regions were below a ratio of one. For the 25μm samples, the only regions with a growth ratio above one was in the shallower sample. the 25×10μm sample had a ratio of 2.03 for double spaced square pillars and 1.25 for single spaced square pillars. It is important to note that all samples other than the 325μm samples had a growth ratio in the control regions that was relatively close to one, while cell growth on untreated

PEEK had a ratio of cell volume to surface area of 0.48.

Cell Distance to Feature

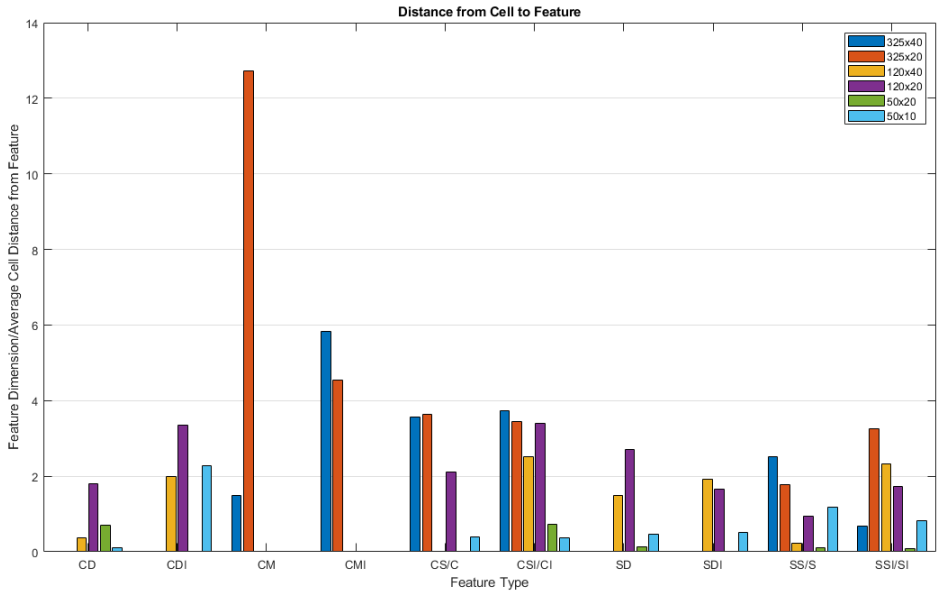


Figure 3.12: Average Cell Distance from Feature

Measurements were taken to determine the influence of features on the location of cells. The measurements used were the percentage of cells on the feature compared to the surrounding area and the average distance of cells to the center of the feature. This revealed that cells were more commonly found growing on larger features then on their smaller counterparts. The greatest percentage of cells on features for $50\mu m$ samples is 20% for the $50\times10\mu m$ single spaced square holes, while the greatest for the $120\mu m$ sample is the $120\times40\mu m$ double spaced square pillar at 71% and 72% for both of the $325\times40\mu m$ square feature regions. Due to smaller features having less room for cells to grow, this is not as strong as an indicator of feature influence as the average distance of cells to features. The distance was non-dimensionalized by dividing the measured feature dimension by the average cell distance to that feature.

Table 3.3: Average Cell Distance

	325×40	325×20	120×40	120×20	50×20	50×10
CD			0.36	1.79	0.71	0.10
CDI			1.99	3.34	0	2.26
CM	1.48	12.71				
CMI	5.82	4.53				
CS/C	3.56	3.63	0	2.10	0	0.39
CSI/CI	3.73	3.44	2.51	3.39	0.72	0.37
SD			0.23	0.93	0.10	1.189
SDI			2.33	1.71	0.08	0.83
SS/S	2.51	1.78	1.49	2.70	0.12	0.46
SSI/SI	0.66	3.25	1.91	1.65	0	0.50

With this ratio, a larger number relates to most cells being closer to features. The ratios of the features are as follows, 2.97 for 325×40μm features, 4.89 for 325×20μm features, 1.35 for 120×40μm features, 2.21 for 120×20μm features, 0.22 for 50×20μm features and 0.76 for 50×10μm features. From these values it can also be generalized that cells are closer to features for shallower samples than for deeper samples. The average distance ratio of double spaced features and the 325μm standard features was 1.51 while the average distance ratio of the single spaced features and the mixed circular features was 2.57. This means that double spaced features had much more influence on cell location.

Discussion

To reiterate, the main objectives in analyzing this data is to establish an absolute best feature for texturing PEEK in bone contacting applications. During the initial contact between tissue and implant the healing bone will resemble cancellous bone with a large number of osteoblast cells and very little hard tissue. This is the situation modeled by plating the samples with the MC3T3 mouse osteoblast cells, and features that encourage good cell viability and a large volume of cell growth will most likely encourage tissue adhesion in healing bone. With this in mind the ideal texture will be one that has the greatest cell growth, given in cell volume, in combination with the greatest cell viability, given in cell counts. The fact that the the feature with the highest cell volume being the $325\times40\mu m$ control volume, and that it out-performed any other control surface including un-patterned control samples, indicates that there is cellular behavior unique to the $325\mu m$ samples. The $325\times40\mu m$ and $325\times20\mu m$ had an average cell growth ratio of 3.04 and 2.74 respectively, in comparison to the control sample average cell growth ratio of 0.48. The layout of the feature patterns places the control regions adjacent to four other textured regions and two on the side as seen in Appendix B. If cells adhered well within these regions, they might grow into one continuous or confluent layer. At this point the cells would start to both form multiple layers and colonize the surrounding areas. Once the cells had formed a large network they are capable of colonizing many surface textures including those that are not initially conducive to cell attachment. If cells were attaching well to the control regions without any assistance from the textured regions, the growth of these control regions should have been the same as the blank PEEK sample. It is interesting to note that only the $325\mu m$ samples had such an extreme increase of cell growth in it's control regions as compared to the other samples. All other samples had control

regions with roughly twice the cell growth as the blank sample.All samples had at least one feature pattern that encouraged cell attachment over control regions, and these cells could then spread into control regions at a similar rate. However for features that grew cells to a confluent layer, the colonization of these control regions was accelerated due to the support of a much larger cellular network. This indicates that a PEEK implant with the $325 \times 40 \mu m$ square pillar surface texture would demonstrate better bone tissue healing than an un-textured implant or an implant patterned with the other surface texture types

Another pattern that emerges is the trend for pillared features to be preferred over hole features. Due to the isotropic nature of the etch in the Aluminum mold, there were no sharp corners. In theory the etch erodes the material in every direction radiating out from the etchant's contact on the metal surface. In practice this happens as small spherical regions are eroded from the surface at multiple points across the contact area. When observed under SEM the average porosity of these expanding erosion pockets was $11.75 \mu m$. Not only does this explain how many of the $10 \mu m$ samples were completely eroded, but it also means that all theoretical right angles were smoothed out as all planes and lines are now made of randomly intersecting semi-spherical surfaces with an average diameter of $11.75 \mu m$. The only place where the surface still resembled a sharp angle was at the surface of the aluminum where it was protected by the photoresist. The tops of holes in the aluminum had more defined corners than the tops of pillars as well, likely because of the reduced mass of the aluminum surrounded by etchant as compared to continuous bulk aluminum surrounding etchant. When pressed into PEEK, the features are mirrored so that holes become pillars and pillars become holes. The base of these new pillars have a more defined, rounded corner than the base of the new holes. After the cells are exposed to Trypsin, they tend to form spheres as they free float above the substrate.

These cells are more likely to attach to the base of pillars then the base of the holes due to the increased available surface area for that initial cell adhesion. Regions that encourage initial cell adhesion will collect a greater number of free floating cells than other regions, which will accelerate the local cell growth. However, just because a hole has less contact area for the initial cell adhesion does not mean that it will repel cellular adhesion, and in some regions more cells randomly adhered to the hole region than the pillar region. The large amount of cellular adhesion in the 120x20μm and 25x10μm double spaced circular hole as compared to the nearly non-existent cellular growth in the corresponding pillar feature is why the double spaced circular holes are the only feature that has a greater average cell growth than it's pillar counterpart across all sample sizes. The greater adhesion in these regions is possibly random and does not break the overall trend.

Another trend to discuss is the increase in cellular growth for shallower features than for deeper features. For the 120μm, 50μm and 25μm features, the shallower feature had both a larger cell volume and a larger cell count. The ratio of live to dead cells does not exhibit this trend but the low cell count for the 50μm and 25μm feature compromises the statistical importance of the ratio instead of the raw cell count, especially for the 50x20μm and 25μm features. For smaller features this is likely because deeper features had less definition in their shape due longer exposure to the isotropic etchant. This means there is very little surface area for cell adhesion during the initial plating. For small enough features, such as the 10μm or 25μm samples, this etchant can completely erode the feature. The resultant regions are very similar to the etched control region populated with randomly distributed 10μm features from the etch defects imprinting into the PEEK. More importantly, the deeper samples for the 50μm and 25μm samples are 20μm deep as opposed to 10μm deep. At this scale, using an assumed cell size of 20-60 μm across and 5-10μm in

depth, cells might be able to compensate for a depth change of 5 or 10μm without undue stress on a cell. However the 20μm edge is enough to disrupt the expansion of a single cell but not deep enough to offer a continuous surface on which to grow. This means that cells growing on a 20 or 40μm feature would need to bend along the top or bottom of a feature adding additional internal stress.

Table 3.4: Average Cell Growth with Respect to Shape

Circular	**Square**
1.06	1.32
Circular Hole	**Circular Pillar**
1.08	1.04
Square Hole	**Square Pillar**
0.90	1.82

As mentioned above, with the isotropic etch rounding all corners on the mold, the ability to test sharp corners against curves was lost in the square and circular features. There is still value in comparing them due to cells growing on a straight wall as opposed to cells growing on curves and it did seem to have an effect. Square Pillars were the feature that had the greatest difference when compared to circular features with an average cell growth ratio of 1.82 while compared to 1.06 for all circular features. the other textures had similar growth ratios as can be seen in Table 3.4. The effects of straight walls is most prominent in larger features and can be seen in some of features with the largest amount of cell growth. Looking at Table 3.2, the 325μm square pillar features have the greatest cell growth for all non control regions. The 120×20μm feature has its largest growth ratio on the double spaced square pillar region at 3.70 and a growth ratio of 2.35 for the single spaced square pillars. These

larger square pillars might encourage cell adhesion of circular pillars due to cells being caught on a flat wall that would otherwise deflect from a curved wall during initial cell adhesion.

The most immediate trend is that cell growth, cell count and proximity to feature is highest at larger features than smaller features. The curves of features for larger features is greater than the curve for smaller features, especially after the effects of the aluminum etch. As cells attach to features, they conform to the surface including any bends in the substrate. For smaller features, cells that attach near a feature and attempt to grow over it need to bend around the curve of the feature as well as having a bend for the base and top of a feature. In addition those base and top bends are less severe for the larger features as the resolution was better for larger features and the greater mass of aluminum in each feature resists the etch. This is why the $120\times20\mu m$ sample has greater cell growth than the smaller $20\mu m$ features, both the curve around the feature, at the top, and at the base of each feature is less sever than for smaller features reducing the internal stress of attached cells. This effect is even grater for $325\mu m$ features to the point where the deeper features had greater cell growth than the shallow features. For these large features the contact area offered by the smoothed corners of the base and gradual wall curve overcame the internal stresses in attached cells as opposed to the severe corners and wall curves in smaller features causing enough internal cell stress to repeal initial adhesion. Cells that have good initial adhesion can adapt to high internal stress and spread into regions that did not encourage adhesion.

CONCLUSION

In conclusion, statistical analysis indicates that There was a greater number of live cells on 120 and 325 μm samples than on un-textured control samples. Other feature characteristics seemed to have an effect on average cell growth but did not statistically change cell numbers from the un-textured control samples. The percentage of dead to live cells did not change significantly from and sample suggesting that all surface textures had the same effect on cell vitality, just increasing the number of cells on larger surface features.

Comparing the average cell growth values between features leads to some speculation on how cells may be behaving during the initial adhesion phase but without direct observation until 72 hours or more after plating, no concrete conclusion can be made for the adhesion strength of cells to the material. All cells imaged are assumed to be well adhered due to the number of rinses the sample undergoes before imaging, but there is no data for the first few hours of adhesion.

The following is speculation on cellular behavior that could drive cell further hypothesis and research. Larger features had a greater boundary area that helped "catch" suspended cells. For example the $325\mu m$ square feature had a theoretical perimeter of $1300\mu m$ which provides adhesion points for at least 20 osteoblasts, using an estimation of $50\mu m$ cells, the most out of any feature tested. Smaller features do not have as good of a boundary for collecting floating cells. If this has an effect on the initial adhesion, the head start of cells growing on larger features could account for the larger cell counts viewed on these samples. Cell growth averages suggest a few other potential conclusions but these require more research to be proven significant. Square features, single spaced features, and pillars grew more cells than their counterparts. This is not statistically proven but could direct future research.

There are several avenues of future work suggested by these results. The largest feature size available in this experiment was $325\mu m$. Since this size also presented optimal cell growth, larger features should be tested to confirm the optimal feature size for encouraging osteoblast growth on the micron scale. As the best feature was square, the effect of straight walls could have a beneficial effect on initial cell adhesion. Squares with more changes in spacing and rows of raised straight $325\mu m$ ridges should be compared. In addition, manufacture methods should be further developed. If a hot embosser with a higher maximum temperature could be obtained, it would potentially increase the quality of all samples, especially smaller feature samples and possibly effect the observed trends. Using pure Al would also potentially improve the feature resolution on the smaller end of the experimental parameter space. In addition, using a substrate or etching method that enables anisotropic etching to create the mold, would provide straighter walls as compared to the sloped walls created with this method. Laser or plasma etched molds could control the wall slope and could form another feature property to optimize.

The micron-scale surface texturing studied in this work is designed to be combined with other techniques, including nano-scale patterning, that could improve osseointegration of PEEK in humans. Optimized patterns should be tested with human cells to insure similar behavior to the MC3T3 cell. If results are consistent with the results shown here in-vivo experiments should be designed with this surface feature. This should be compared with hydroxyapatite coating, hydrogel coating and oxygen plasma etching both on control samples and layered on this texture. This texture was designed to be used in conjunction with other successful osseointegrating methods and needs to be tested alongside them. The effect of osteoblast adhesion when challenged with bacteria common from surgery infections such as *S. aureus* should be recorded as well. The use of antibacterial coatings could be layered

with other techniques described and challenged as well. Samples that had poor cell adhesion could be further optimized and tested against other adhesion resistant textures to determine effectiveness when used in this manner.

REFERENCES CITED

[1] C. K. Akkan, M. Hammadeh, S. Brück, H. W. Park, M. Veith, H. Abdul-Khaliq, and C. Aktas. Plasma and short pulse laser treatment of medical grade PEEK surfaces for controlled wetting. *Materials Letters*, 2013.

[2] M. A. Bag and L. M. Valenzuela. Impact of the hydration states of polymers on their hemocompatibility for medical applications: A review, 2017.

[3] D. Cordero, M. López-Álvarez, C. Rodríguez-Valencia, J. Serra, S. Chiussi, and P. González. In vitro response of pre-osteoblastic cells to laser microgrooved PEEK. *Biomedical Materials (Bristol)*, 2013.

[4] A. M. Díez-Pascual, M. Naffakh, M. A. Gómez, C. Marco, G. Ellis, M. T. Martínez, A. Ansón, J. M. González-Domínguez, Y. Martínez-Rubi, and B. Simard. Development and characterization of PEEK/carbon nanotube composites. *Carbon*, 47(13):3079–3090, 2009.

[5] M. L. Goodson, D. Farr, D. Keith, and R. J. Banks. Use of two-piece polyetheretherketone (PEEK) implants in orbitozygomatic reconstruction. *British Journal of Oral and Maxillofacial Surgery*, 50(3):268–269, 2012.

[6] S. Green. Chapter 3 - Compounds and Composite Materials. In S. M. Kurtz, editor, *PEEK Biomaterials Handbook*, Plastics Design Library, pages 23–48. William Andrew Publishing, Oxford, 2012.

[7] J. Khoury, S. R. Kirkpatrick, M. Maxwell, R. E. Cherian, A. Kirkpatrick, and R. C. Svrluga. Neutral atom beam technique enhances bioactivity of PEEK. *Nuclear Instruments and Methods in Physics Research, Section B: Beam Interactions with Materials and Atoms*, 2013.

[8] S. M. Kurtz. Chapter 13 - Applications of Polyaryletheretherketone in Spinal Implants: Fusion and Motion Preservation. In S. M. Kurtz, editor, *PEEK Biomaterials Handbook*, Plastics Design Library, pages 201–220. William Andrew Publishing, Oxford, 2012.

[9] R. Ma and T. Tang. Current strategies to improve the bioactivity of PEEK, 2014.

[10] B. K. D. Ngo and M. A. Grunlan. Protein Resistant Polymeric Biomaterials, 2017.

[11] S. Seaman, P. Kerezoudis, M. Bydon, J. C. Torner, and P. W. Hitchon. Titanium vs. polyetheretherketone (PEEK) interbody fusion: Meta-analysis and review of the literature, 2017.

[12] R. Smeets, B. Stadlinger, F. Schwarz, B. Beck-Broichsitter, O. Jung, C. Precht, F. Kloss, A. Gröbe, M. Heiland, and T. Ebker. Impact of Dental Implant Surface Modifications on Osseointegration, 2016.

[13] H. Sun, J. Chen, X. Han, and H. Liu. Multi-responsive hydrogels with UCST- and LCST-induced shrinking and controlled release behaviors of rhodamine B. *Materials Science and Engineering C*, 2018.

[14] A. Syahrom, M. Al-Fatihhi, M. Szali, J. Muhamad, N. Harun, and A. Öchsner. *Cancellous Bone - Mechanical Characterization and Finite Element Simulation*. 2018.

[15] J. M. Toth. Chapter 7 - Biocompatibility of Polyaryletheretherketone Polymers. In S. M. Kurtz, editor, *PEEK Biomaterials Handbook*, Plastics Design Library, pages 81–92. William Andrew Publishing, Oxford, 2012.

[16] W. Wang and K. W. Yeung. Bone grafts and biomaterials substitutes for bone defect repair: A review, 2017.

[17] T. Wu, J. Zhang, Y. Wang, D. Li, B. Sun, H. El-Hamshary, M. Yin, and X. Mo. Fabrication and preliminary study of a biomimetic tri-layer tubular graft based on fibers and fiber yarns for vascular tissue engineering. *Materials Science and Engineering C*, 2018.

[18] S. Yu, K. P. Hariram, R. Kumar, P. Cheang, and K. K. Aik. In vitro apatite formation and its growth kinetics on hydroxyapatite/ polyetheretherketone biocomposites. *Biomaterials*, 26(15):2343–2352, 2005.

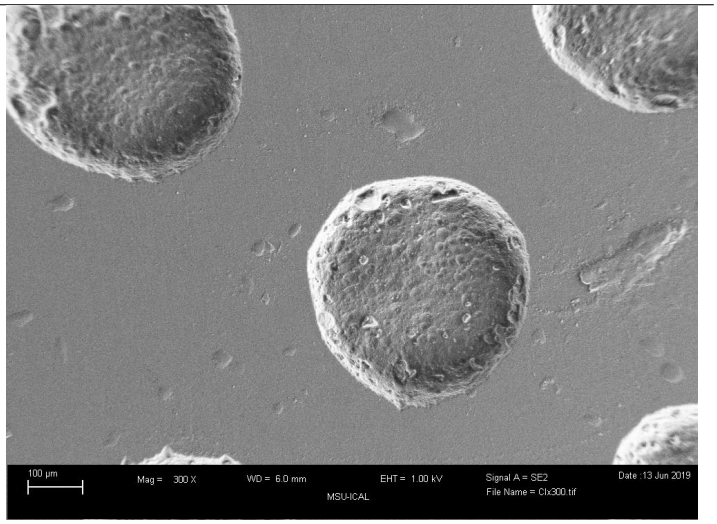
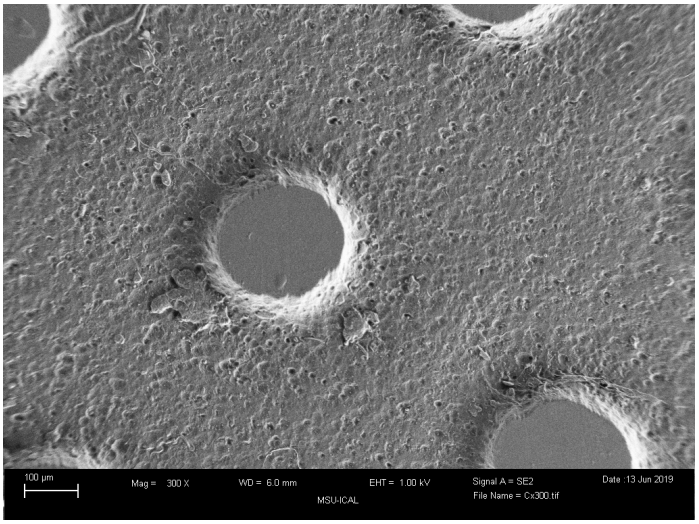
APPENDICES

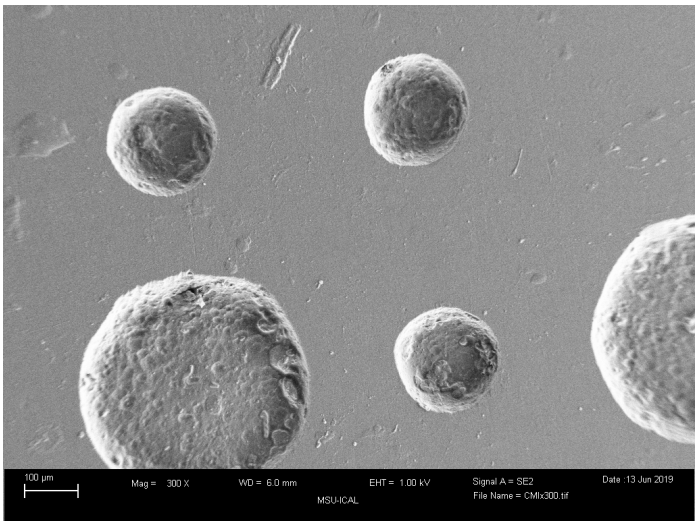
APPENDIX A

SURFACE TEXTURES

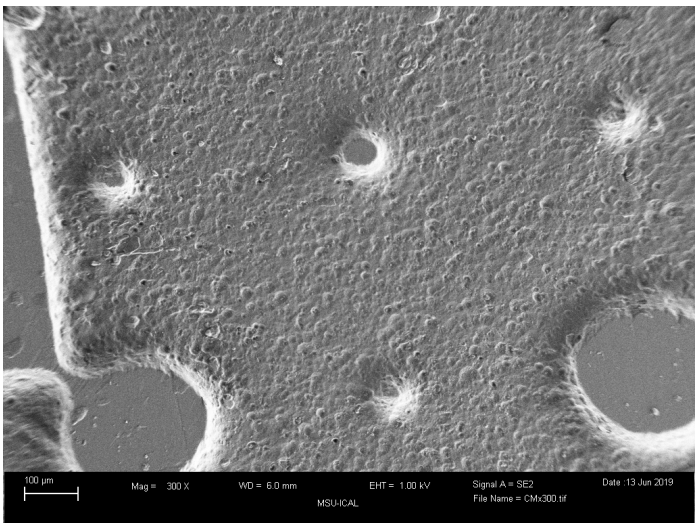
Below is a reference table of all the surface textures as they appear on the Aluminum mold. The PEEK textures are mirrors of these textures, it can be visualized as looking at the PEEK surface texture from underneath. The $25\mu m$ and $10\mu m$ features did not imprint well for every features due to the low hot embossing temperature available and did not always mirror the textures shown here. the $10\mu m$ Square Double Spaced Pillar features are the worst features for poor etch resolution, leaving irregular patterns with missing features.

Table A.1: Surface Texture Types as seen under SEM on Al Mold

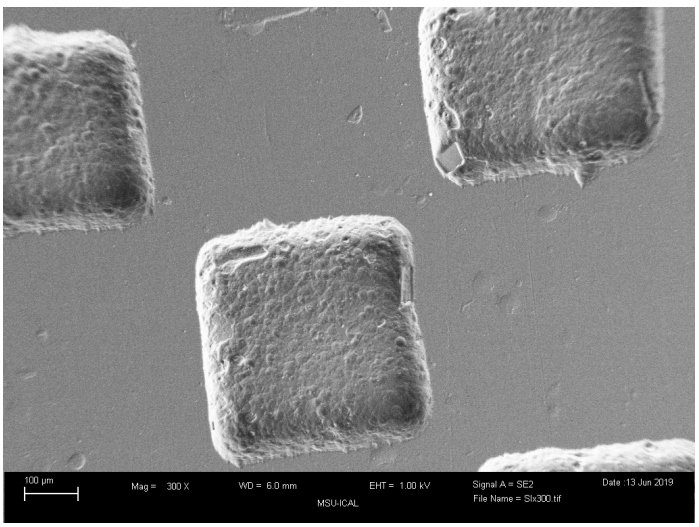
$325\times40\mu m$ Circular Pillars	
$325\times40\mu m$ Circular Holes	



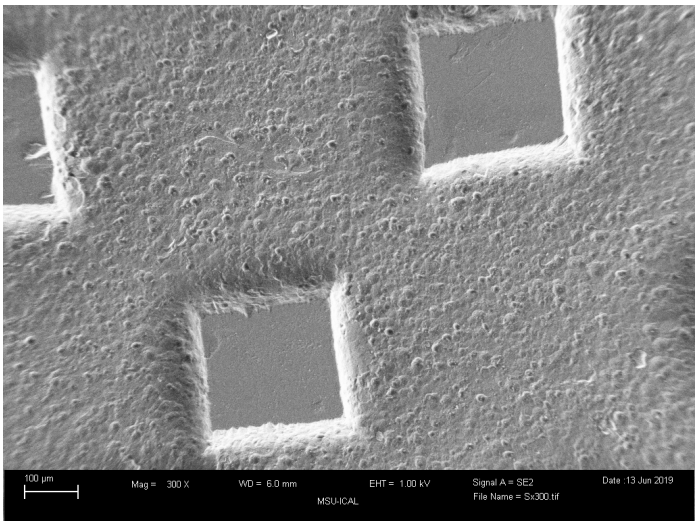
$325\times40\mu m$ Circular Mixed Pillars



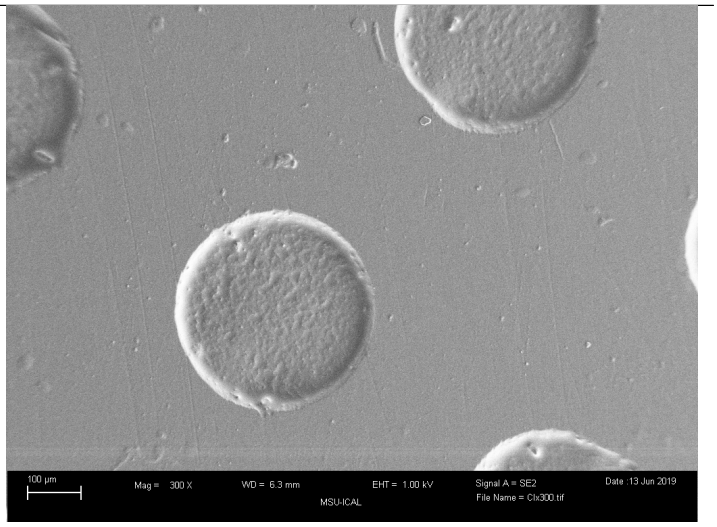
$325\times40\mu m$ Circular Mixed Holes



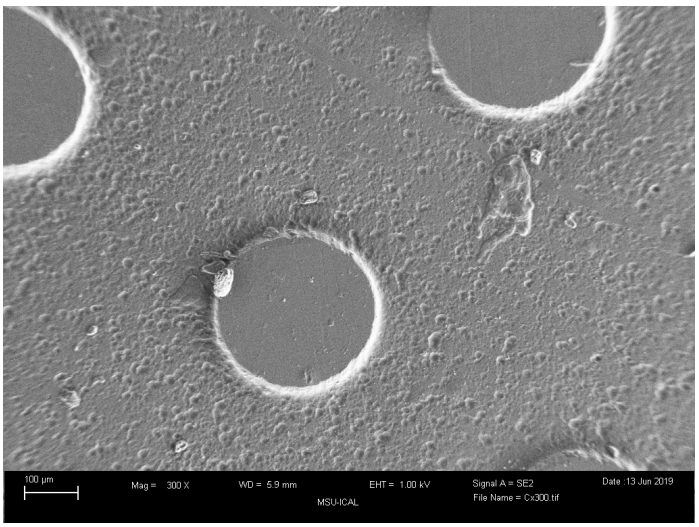
$325\times40\mu m$ Square Pillars



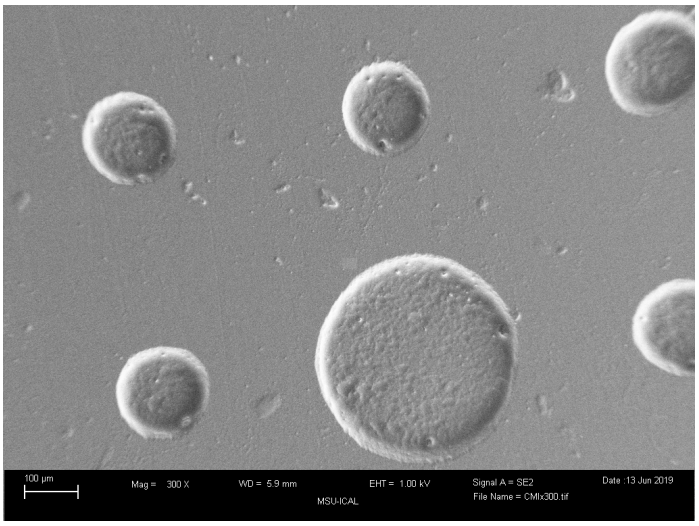
$325\times40\mu m$ Square Holes



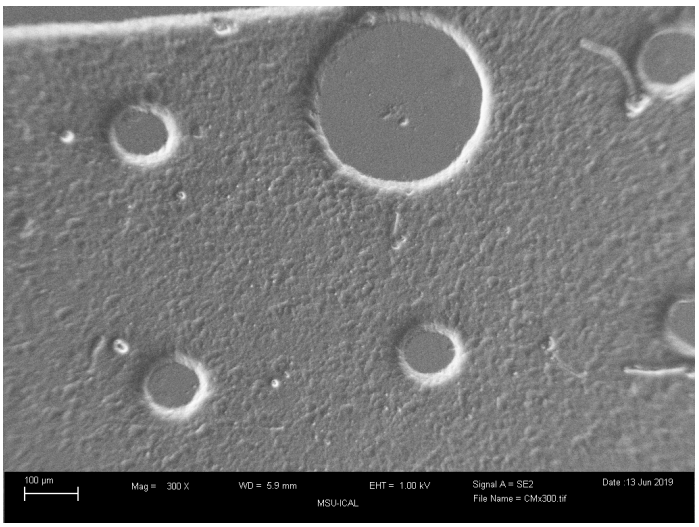
$325\times20\mu m$ Circular Pillars



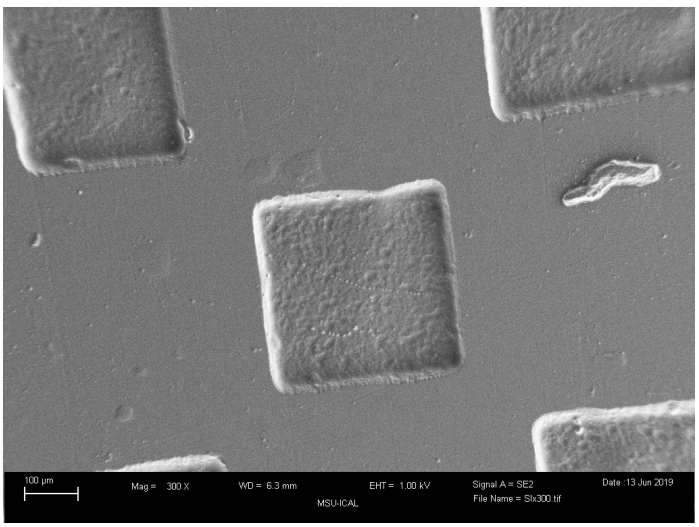
$325\times20\mu m$ Circular Holes



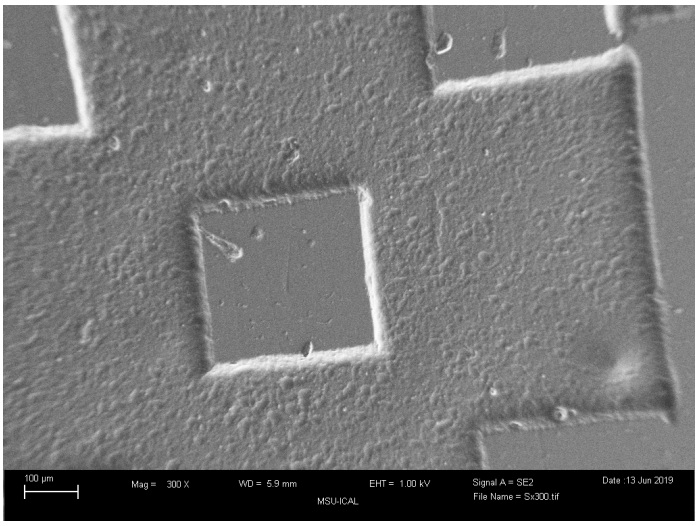
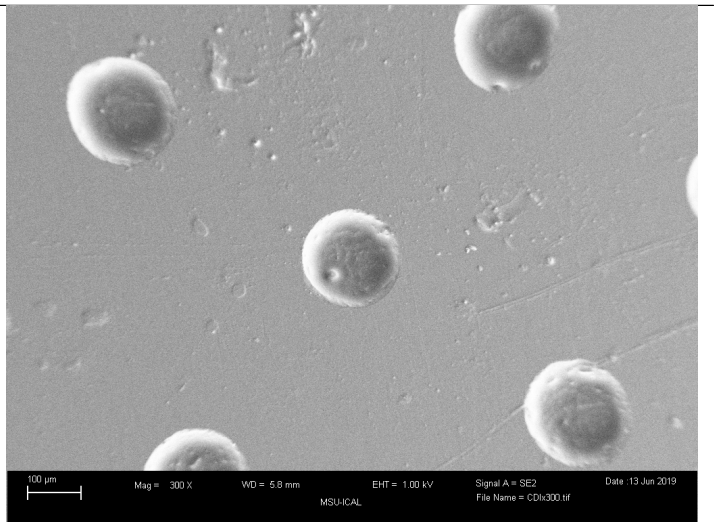
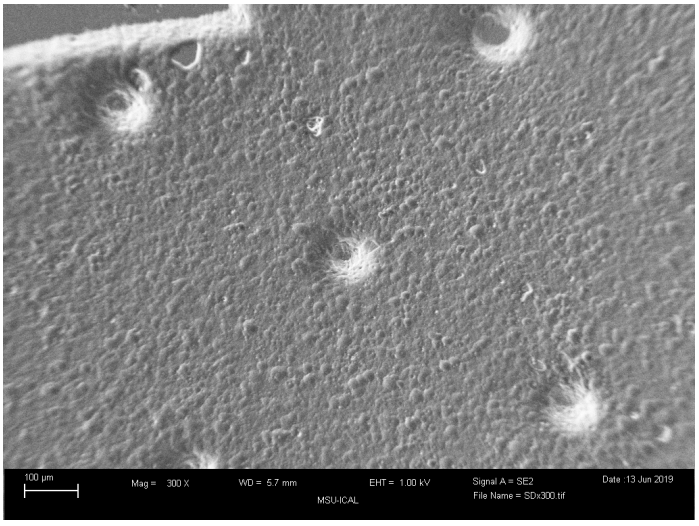
$325\times20\mu m$ Circular Mixed Pillars

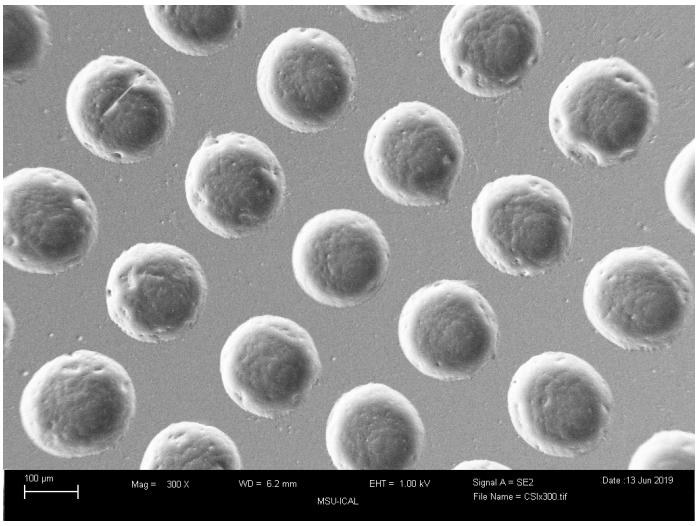


$325\times20\mu m$ Circular Mixed Holes

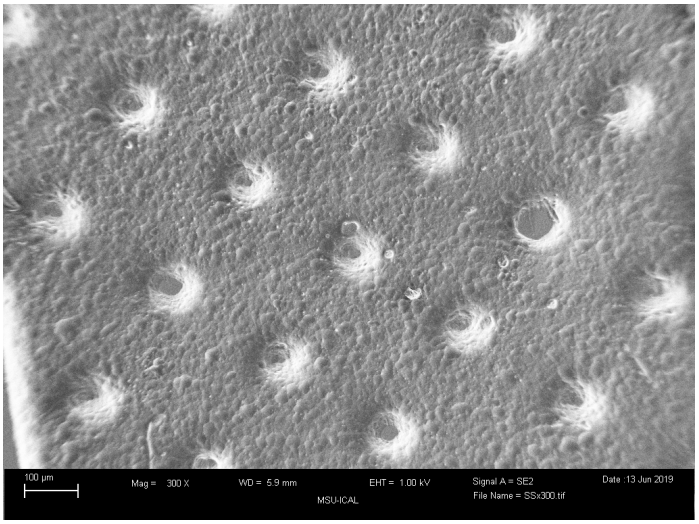


$325\times20\mu m$ Square Pillars

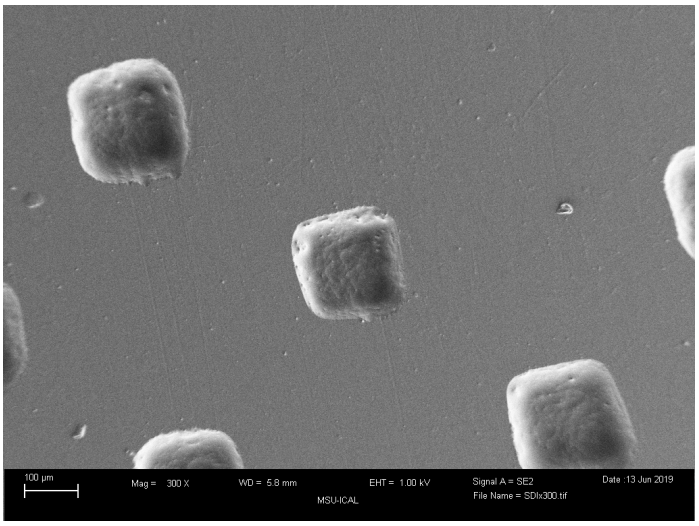
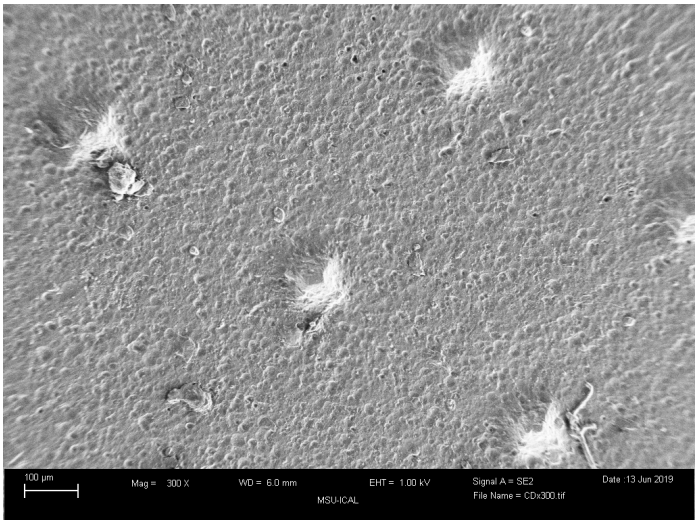
$325\times20\mu m$ Square Holes	
$120\times40\mu m$ Circular Double Spaced Pillars	
$120\times40\mu m$ Circular Double Spaced Holes	

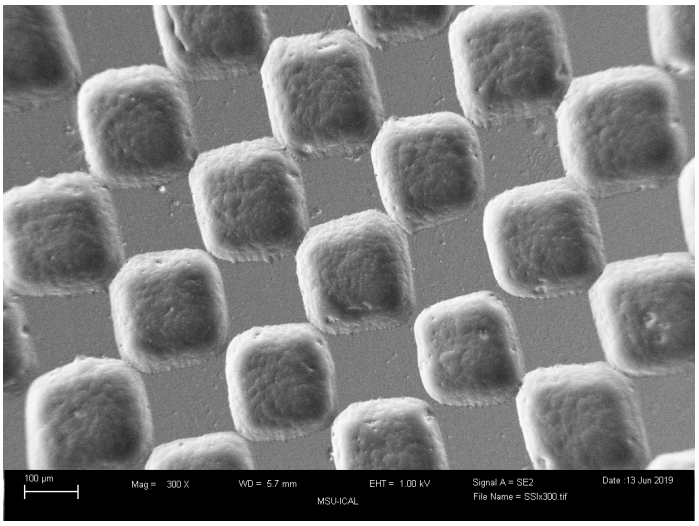
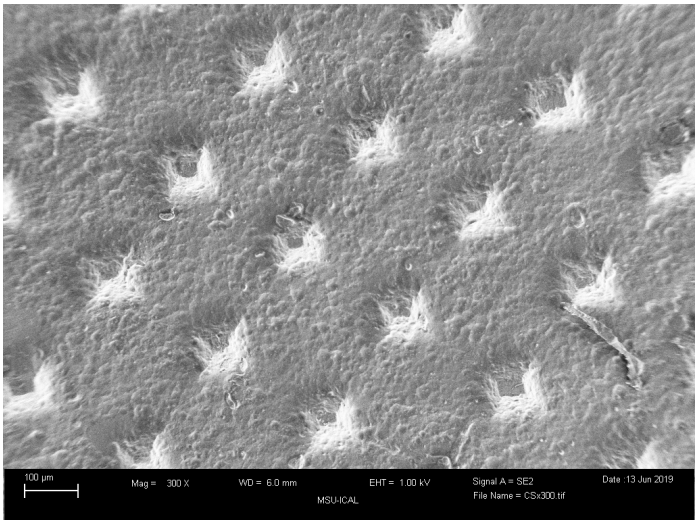


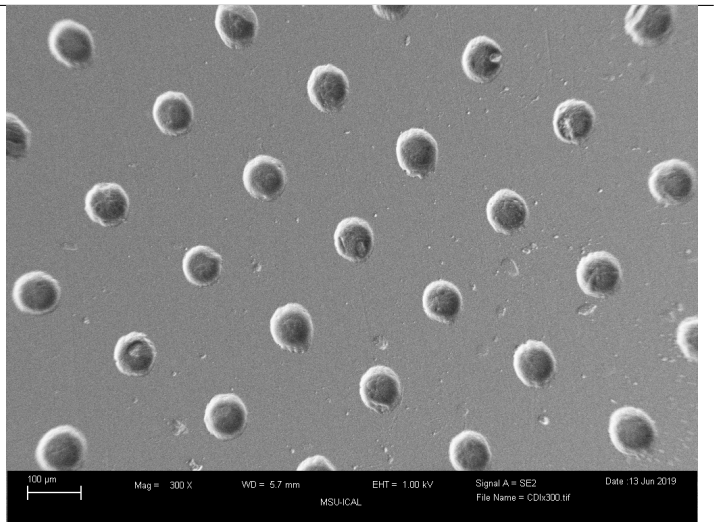
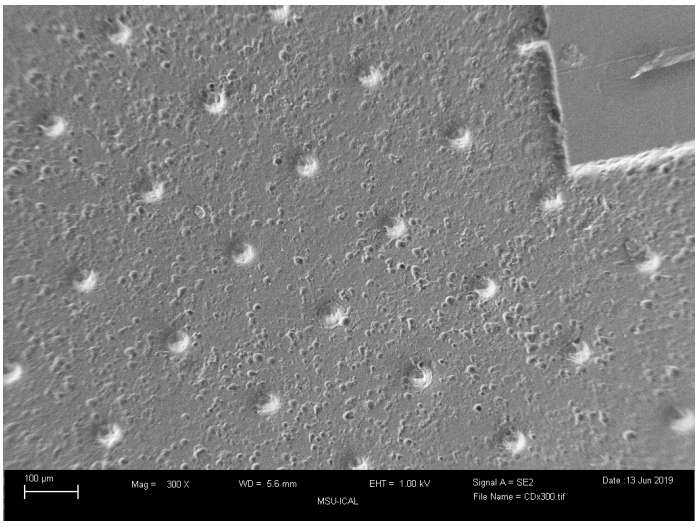
$120\times40\mu m$ Circular Single Spaced Pillars

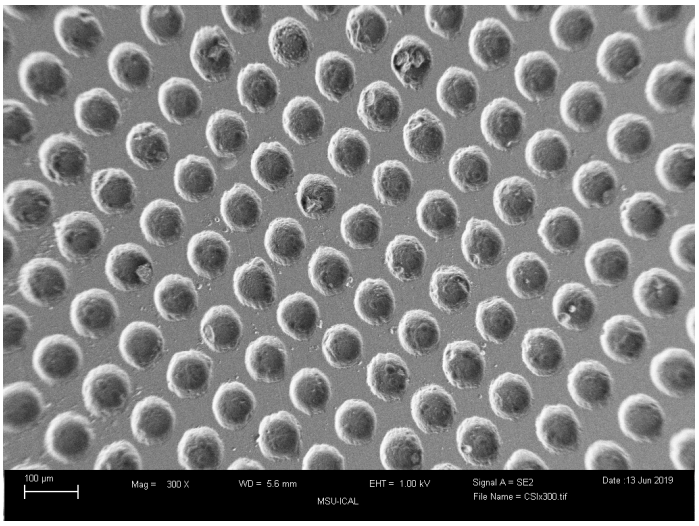


$120\times40\mu m$ Circular Single Spaced Holes

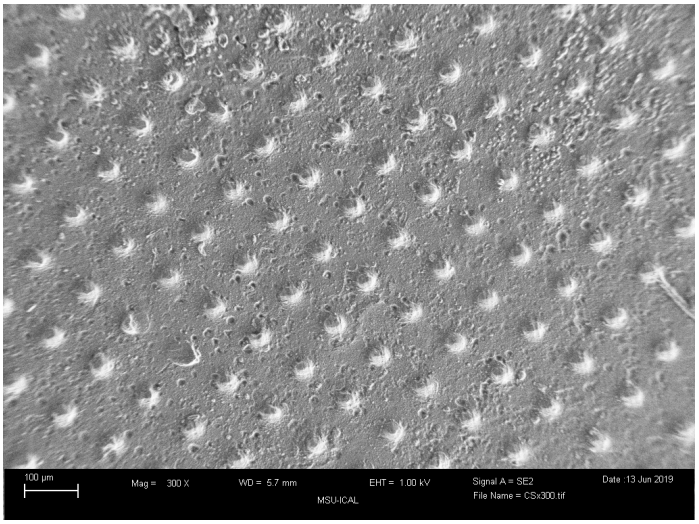
$120\times40\mu m$ Square Double Spaced Pillars	
$120\times40\mu m$ Square Double Spaced Holes	

$120\times40\mu m$ Square Single Spaced Pillars	
$120\times40\mu m$ Square Single Spaced Holes	

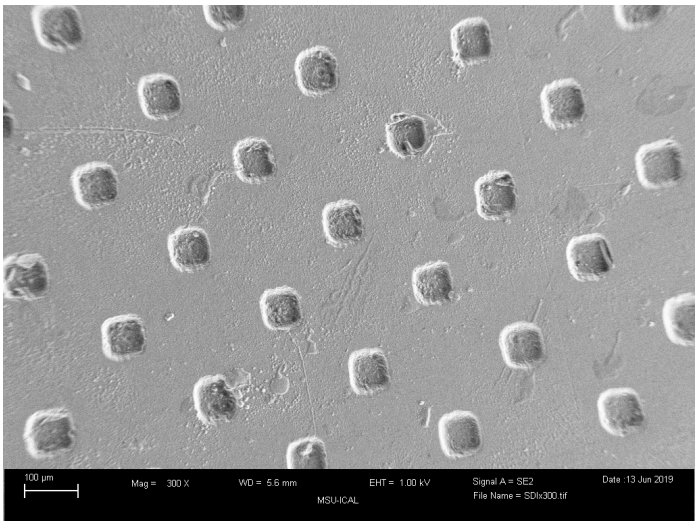
$50\times20\mu m$ Circular Double Spaced Pillars	
$50\times20\mu m$ Circular Double Spaced Holes	



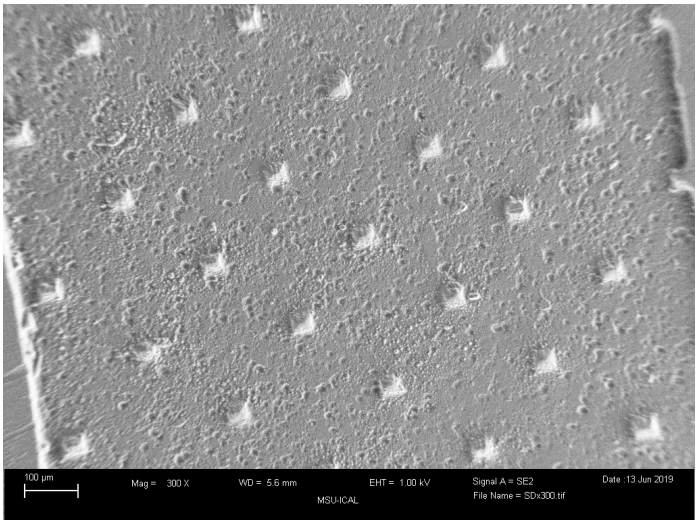
$50\times20\mu m$ Circular Single Spaced Pillars



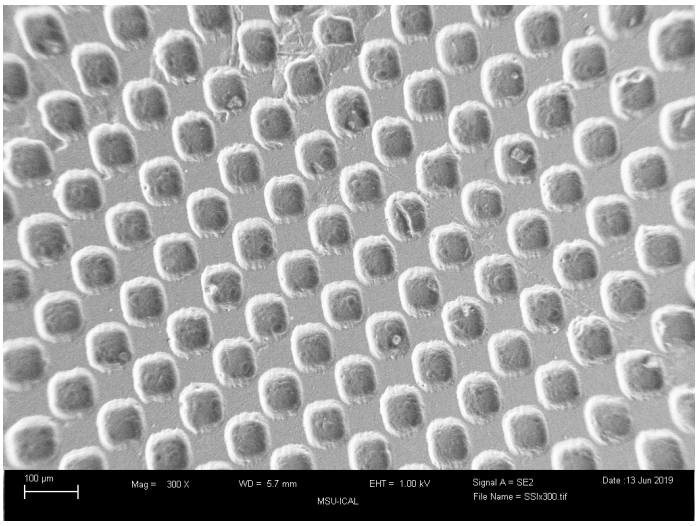
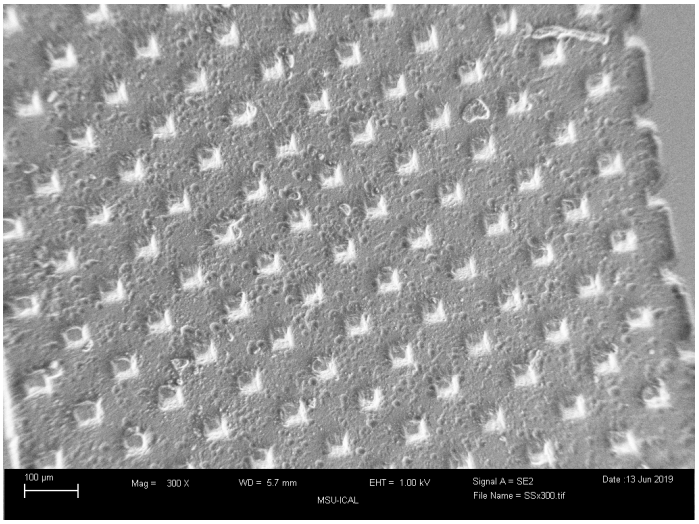
$50\times20\mu m$ Circular Single Spaced Holes

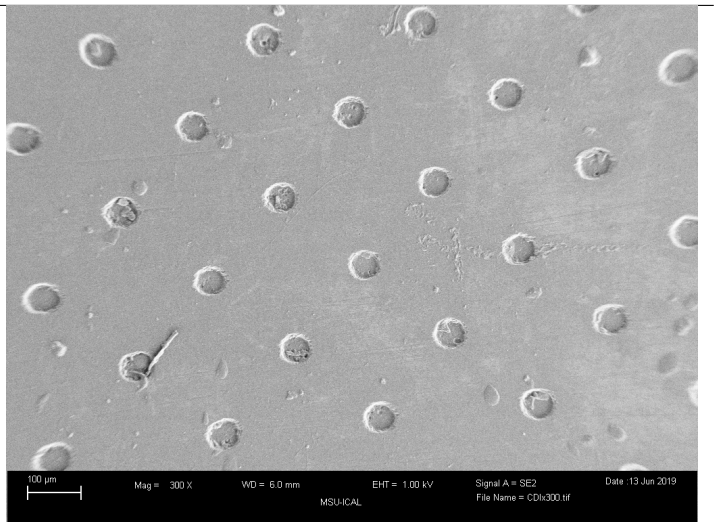
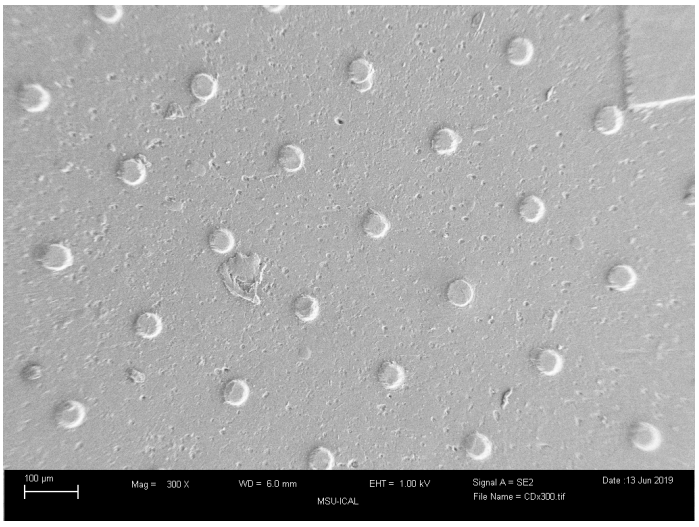


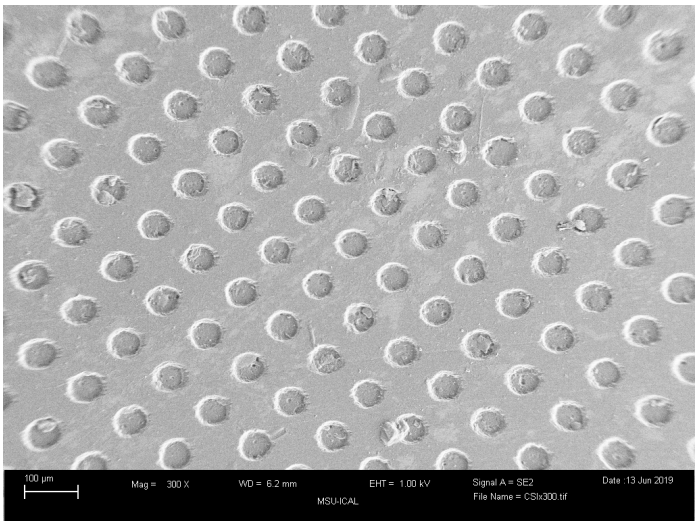
$50\times20\mu m$ Square Double Spaced Pillars



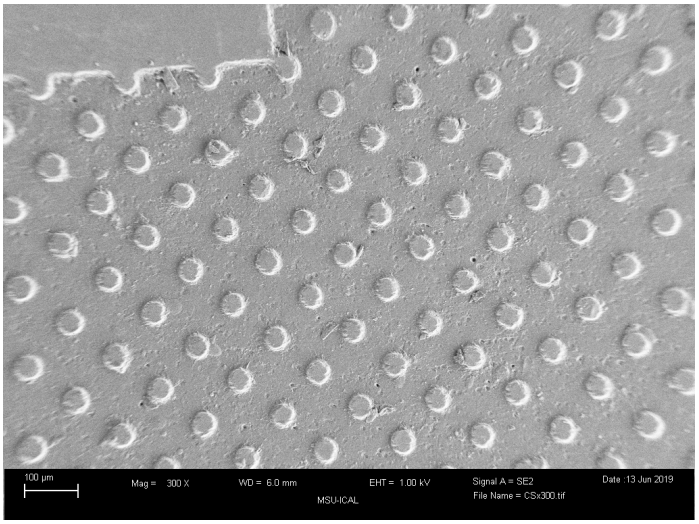
$50\times20\mu m$ Square Double Spaced Holes

$50\times20\mu m$ Square Single Spaced Pillars	
$50\times20\mu m$ Square Single Spaced Holes	

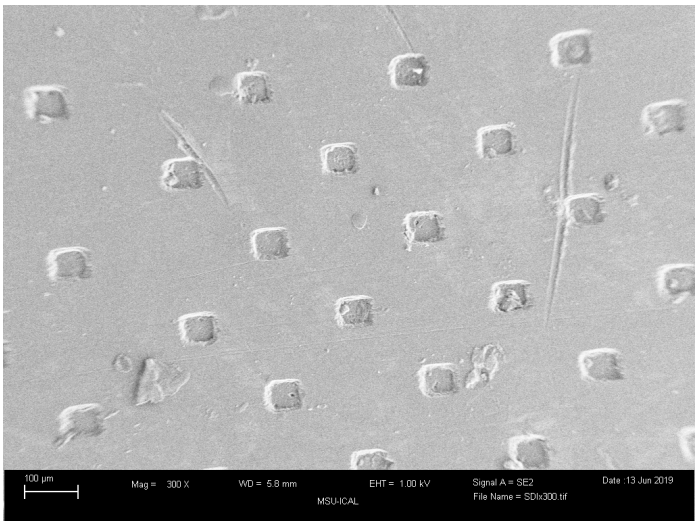
$50\times10\mu m$ Circular Double Spaced Pillars	
$50\times10\mu m$ Circular Double Spaced Holes	



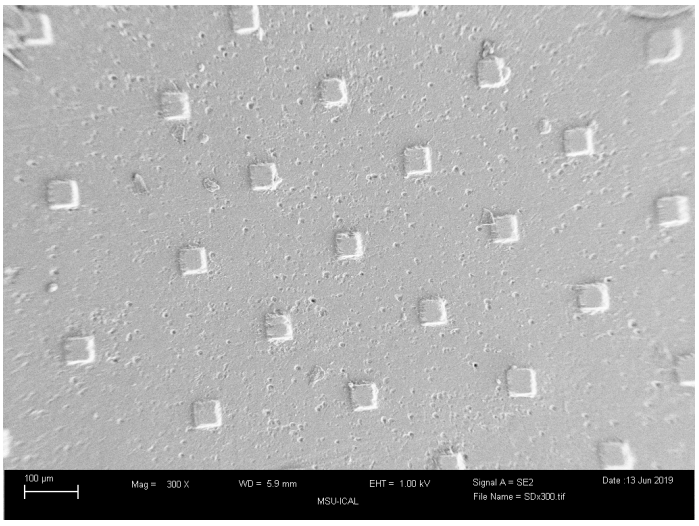
$50\times10\mu m$ Circular Single Spaced Pillars



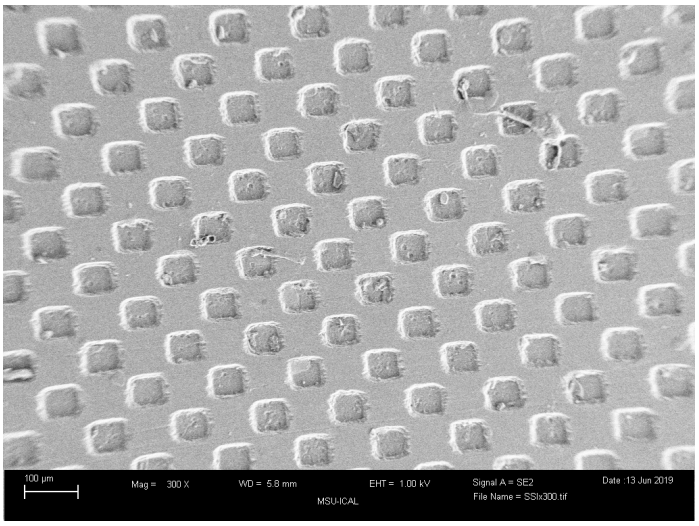
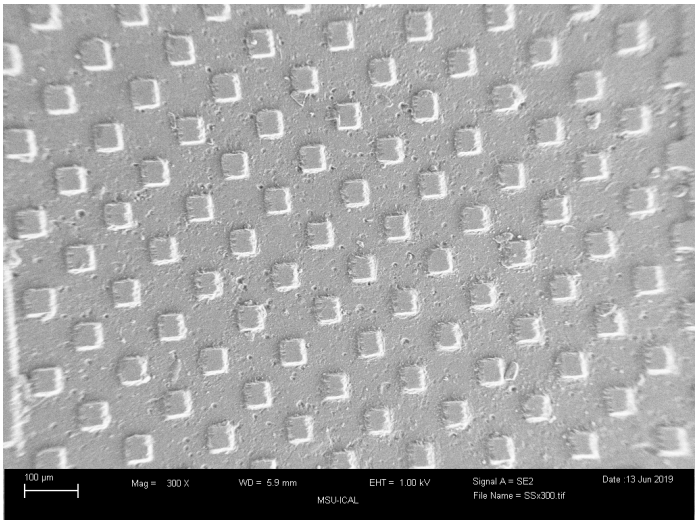
$50\times10\mu m$ Circular Single Spaced Holes

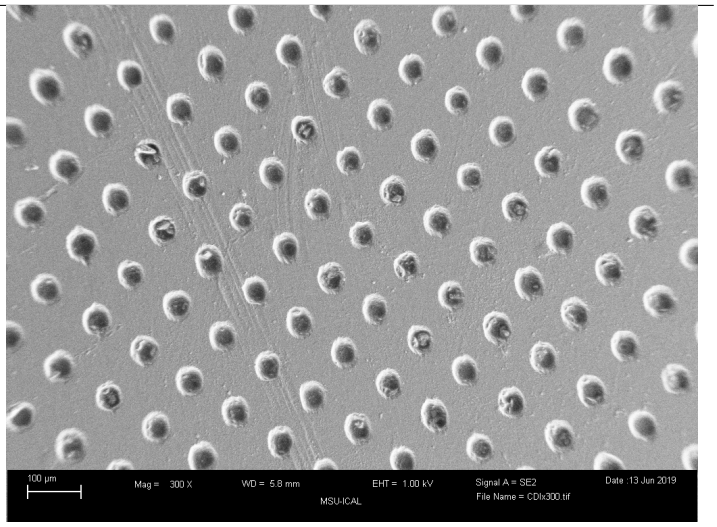
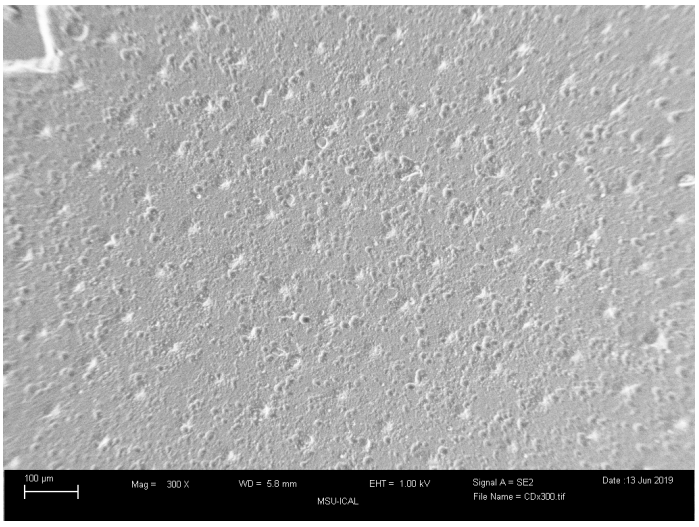


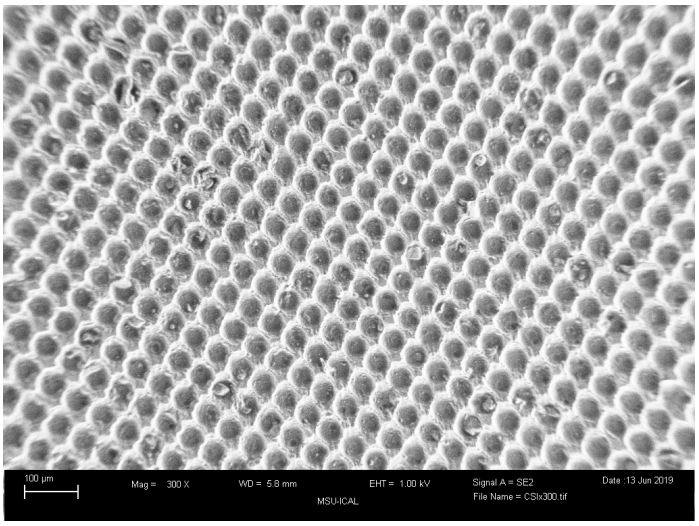
$50\times10\mu m$ Square Double Spaced Pillars



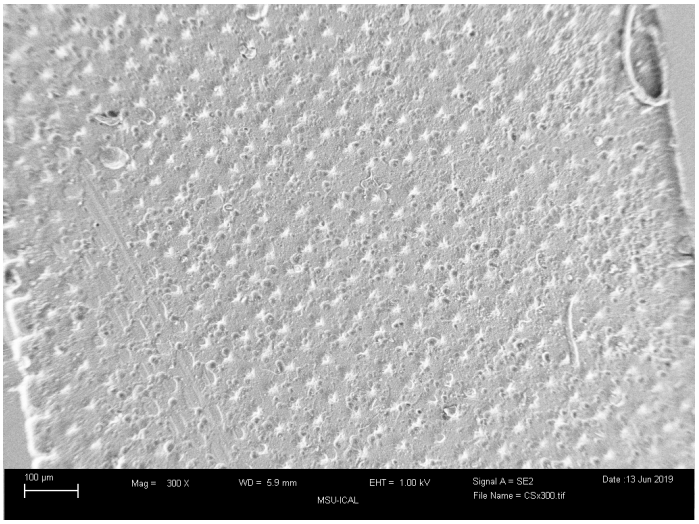
$50\times10\mu m$ Square Double Spaced Holes

$50\times10\mu m$ Square Single Spaced Pillars	
$50\times10\mu m$ Square Single Spaced Holes	

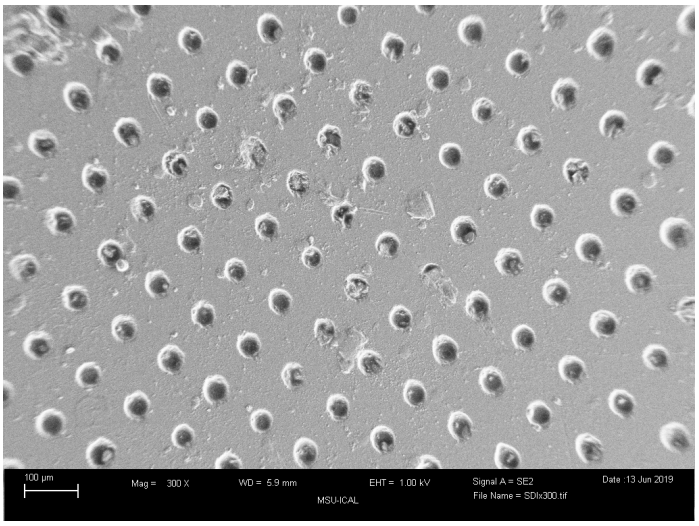
$25\times20\mu m$ Circular Double Spaced Pillars	
$25\times20\mu m$ Circular Double Spaced Holes	



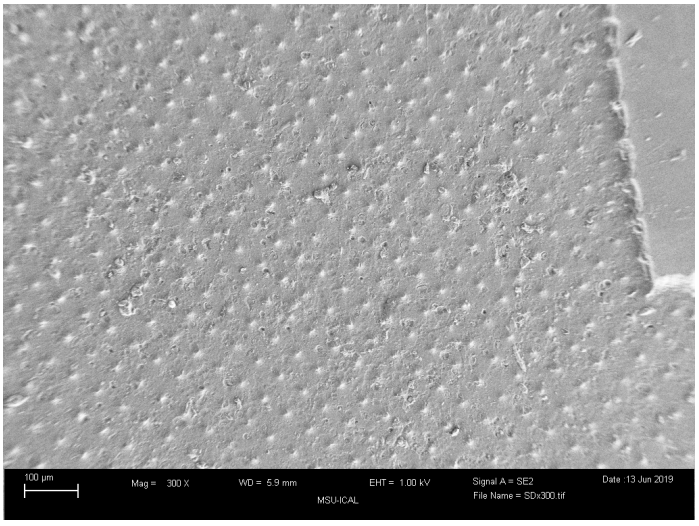
$25\times20\mu m$ Circular Single Spaced Pillars



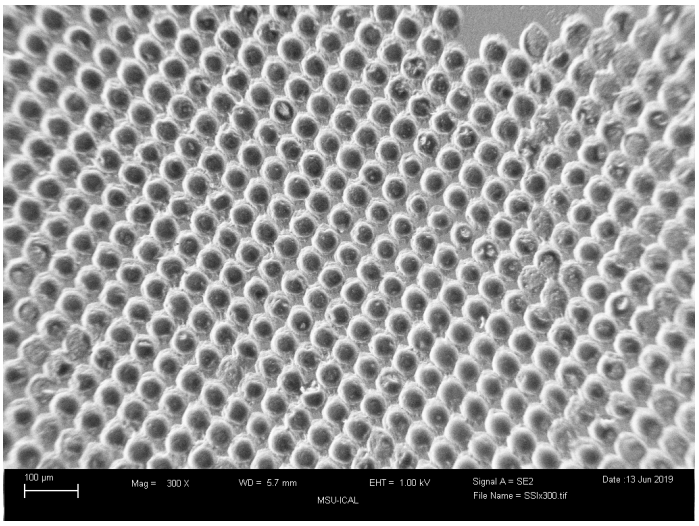
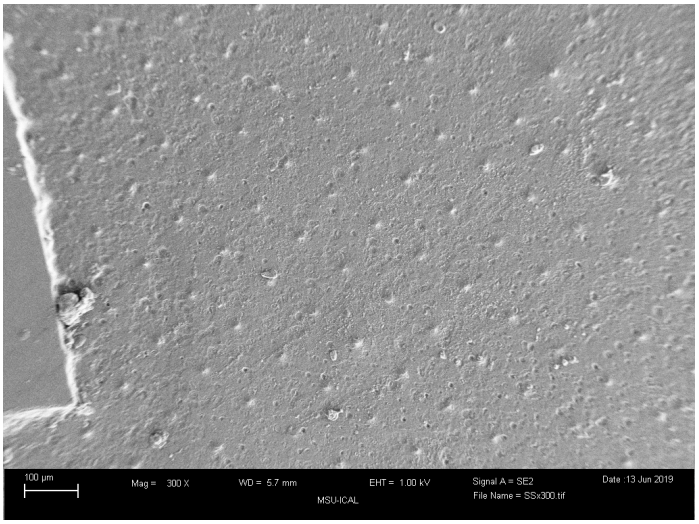
$25\times20\mu m$ Circular Single Spaced Holes

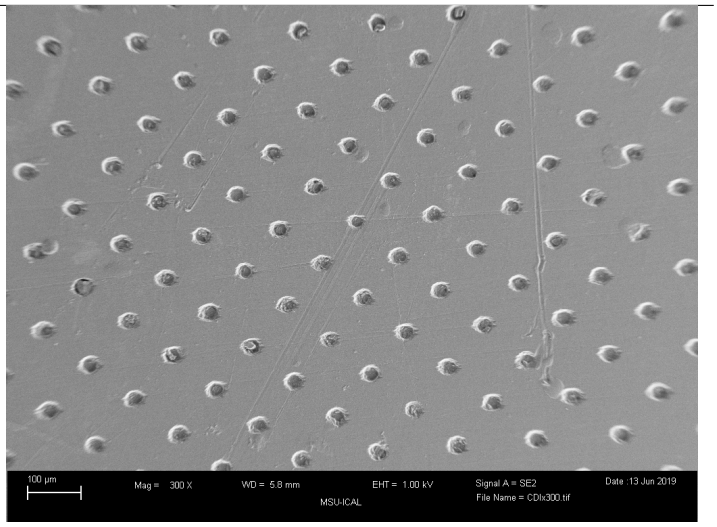
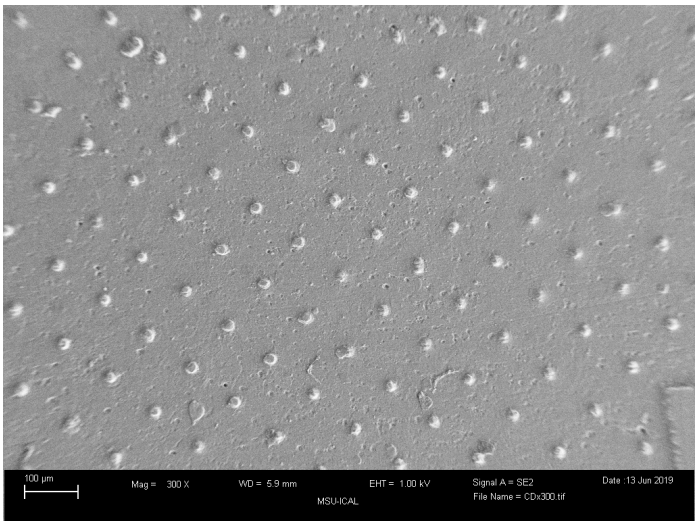


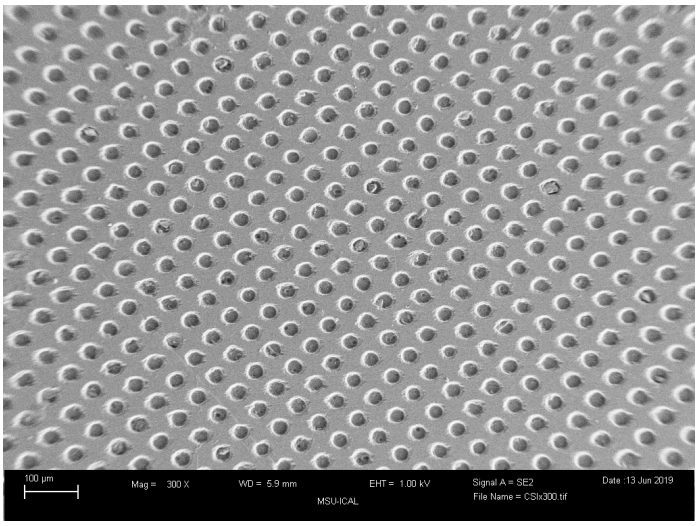
$25\times20\mu m$ Square Double Spaced Pillars



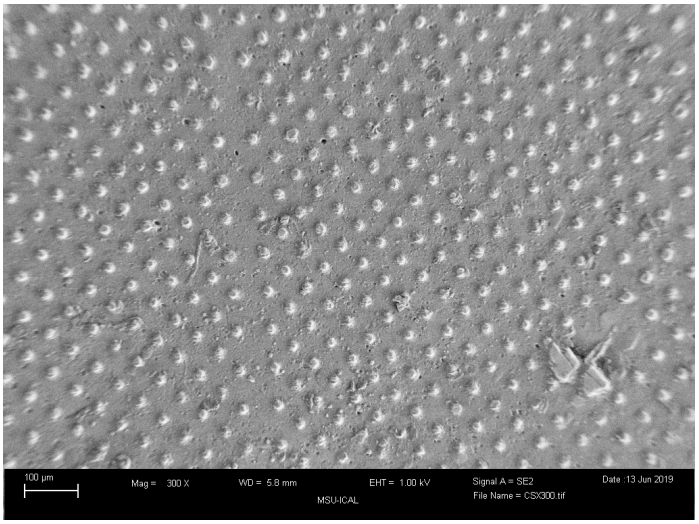
$25\times20\mu m$ Square Double Spaced Holes

$25\times20\mu m$ Square Single Spaced Pillars	
$25\times20\mu m$ Square Single Spaced Holes	

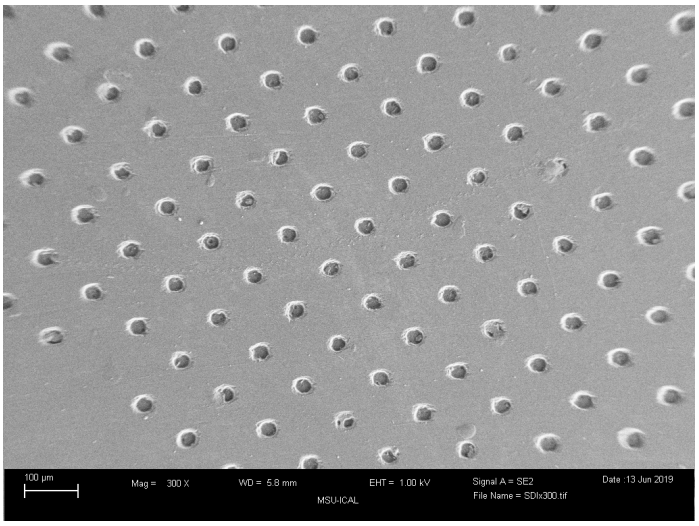
$25\times10\mu m$ Circular Double Spaced Pillars	
$25\times10\mu m$ Circular Double Spaced Holes	



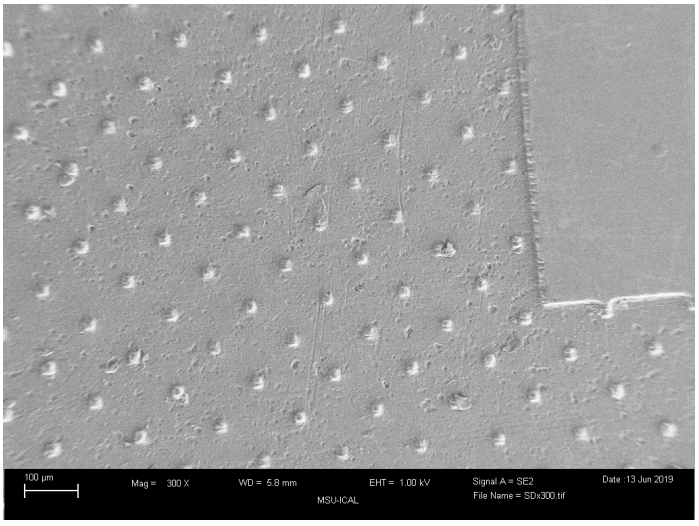
$25\times10\mu m$ Circular Single Spaced Pillars



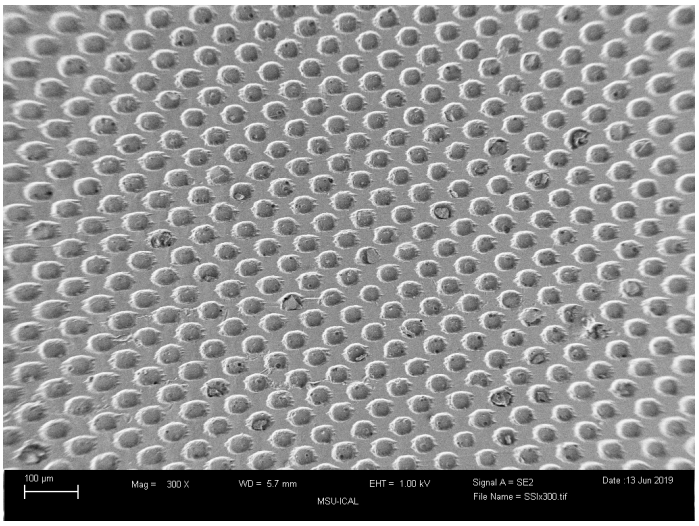
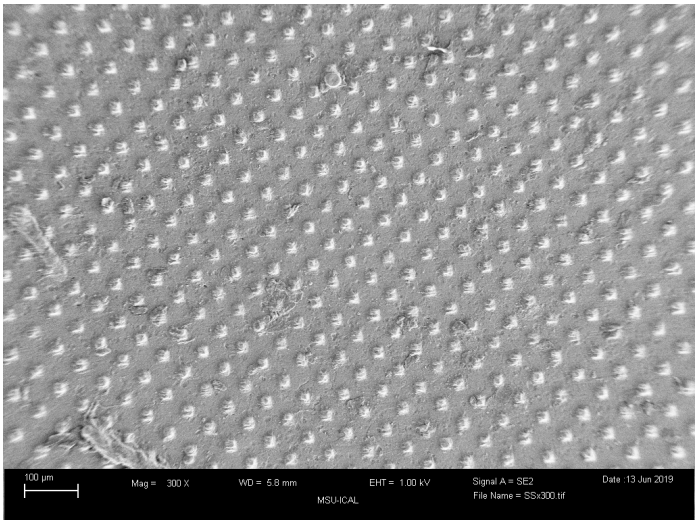
$25\times10\mu m$ Circular Single Spaced Holes

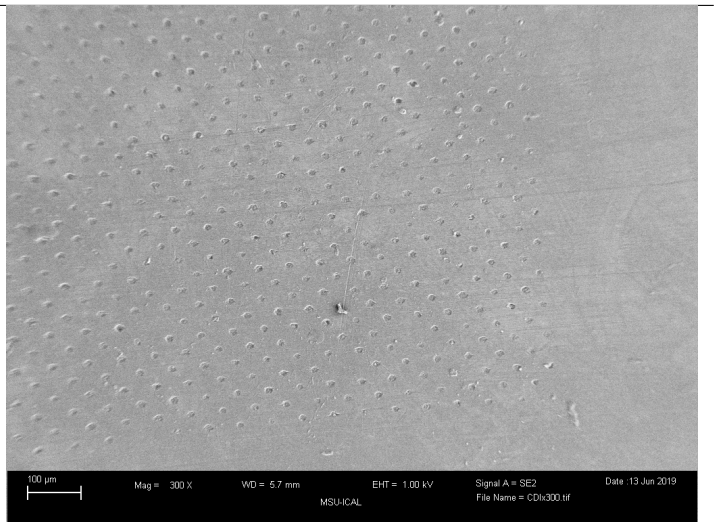
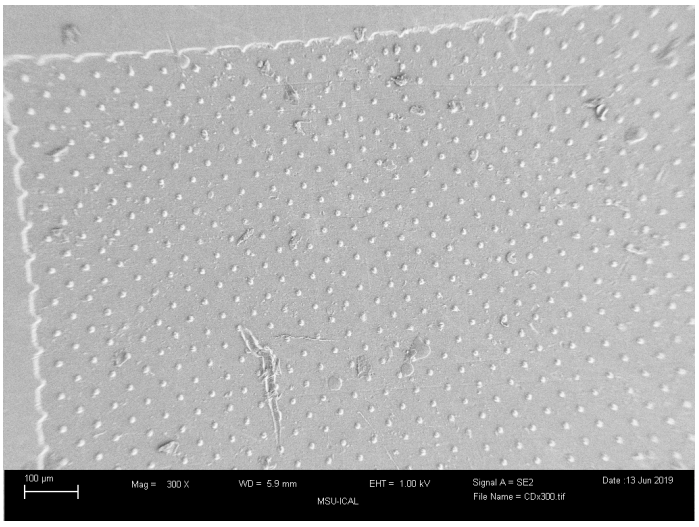


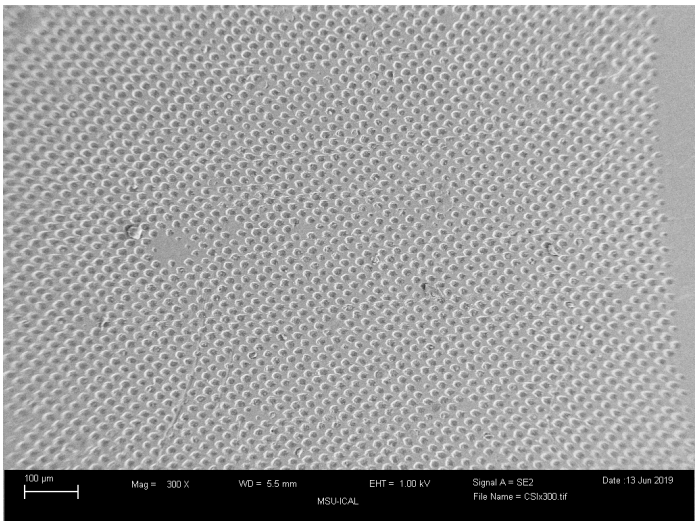
$25\times10\mu m$ Square Double Spaced Pillars



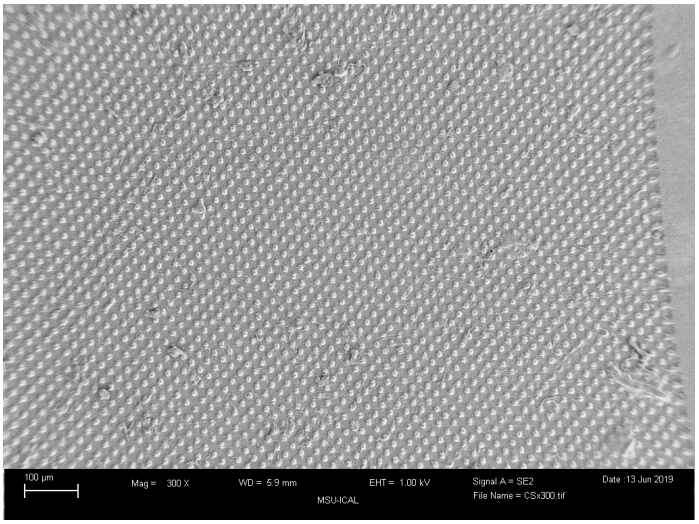
$25\times10\mu m$ Square Double Spaced Holes

$25\times10\mu m$ Square Single Spaced Pillars	
$25\times10\mu m$ Square Single Spaced Holes	

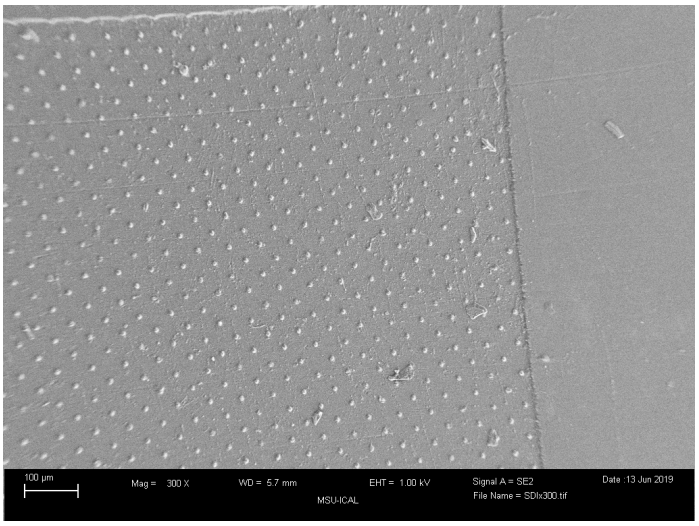
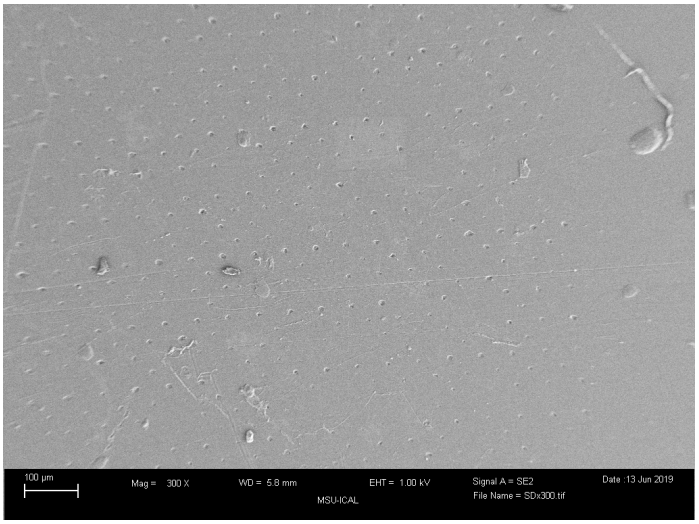
$10\times10\mu m$ Circular Double Spaced Pillars	
$10\times10\mu m$ Circular Double Spaced Holes	

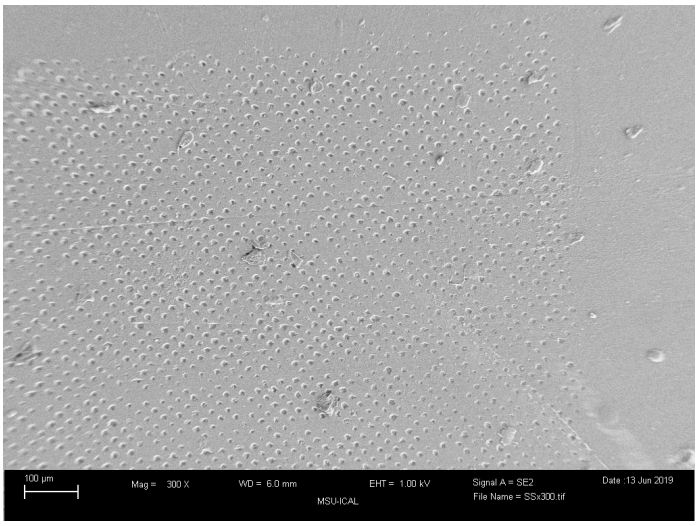
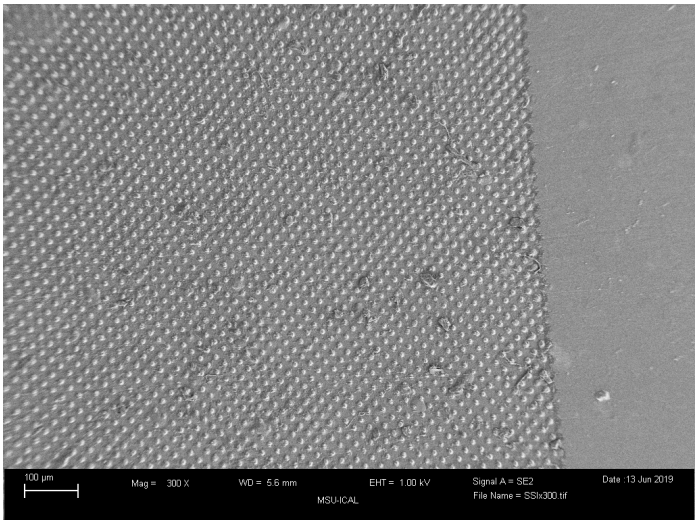


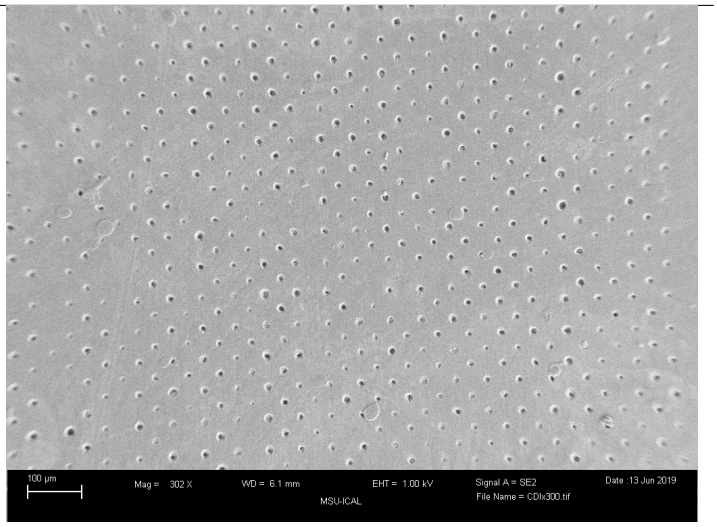
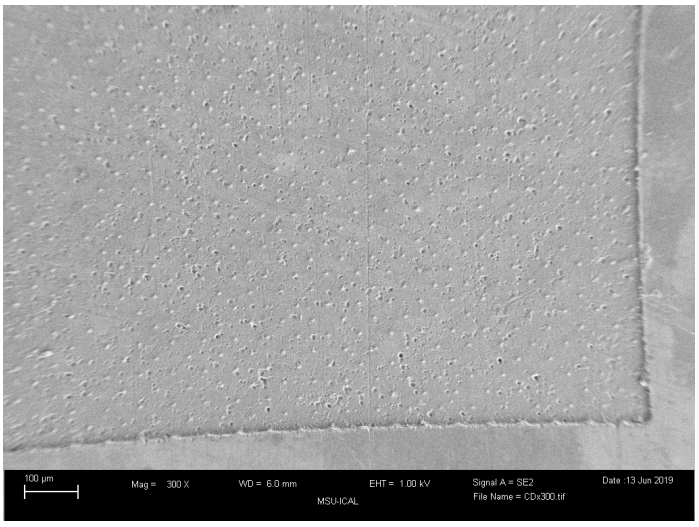
$10\times10\mu m$ Circular Single Spaced Pillars

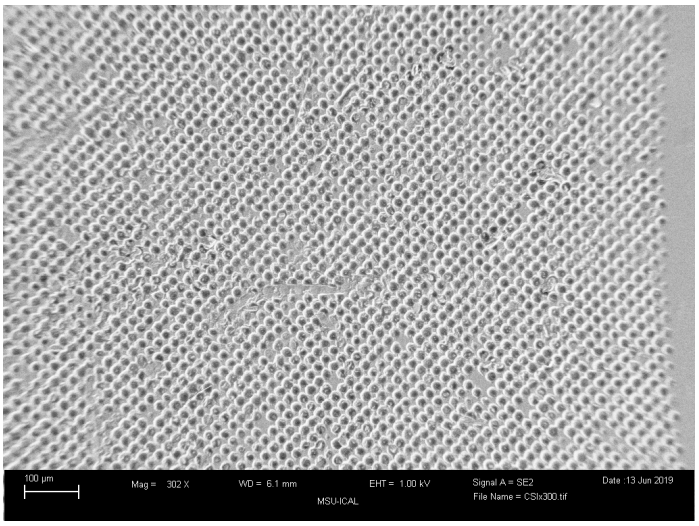


$10\times10\mu m$ Circular Single Spaced Holes

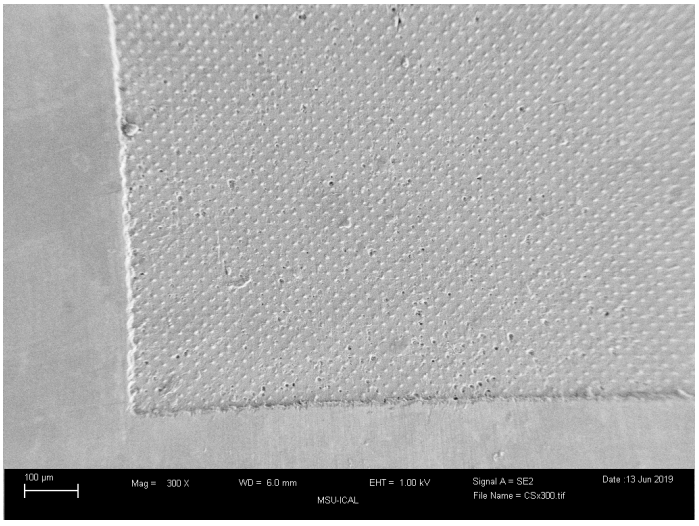
$10\times10\mu m$ Square Double Spaced Pillars	
$10\times10\mu m$ Square Double Spaced Holes	

$10\times10\mu m$ Square Single Spaced Pillars	
$10\times10\mu m$ Square Single Spaced Holes	

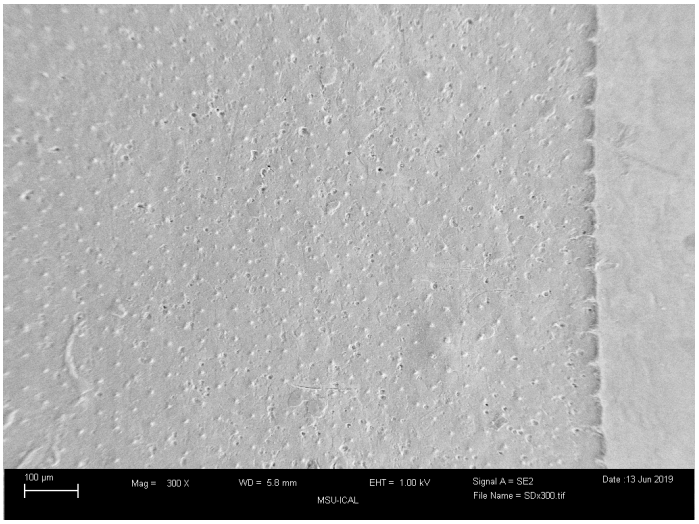
$10\times5\mu m$ Circular Double Spaced Pillars	
$10\times5\mu m$ Circular Double Spaced Holes	

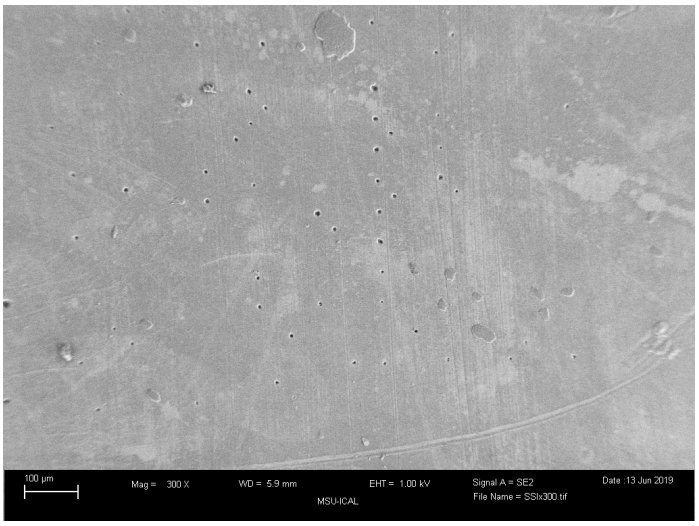
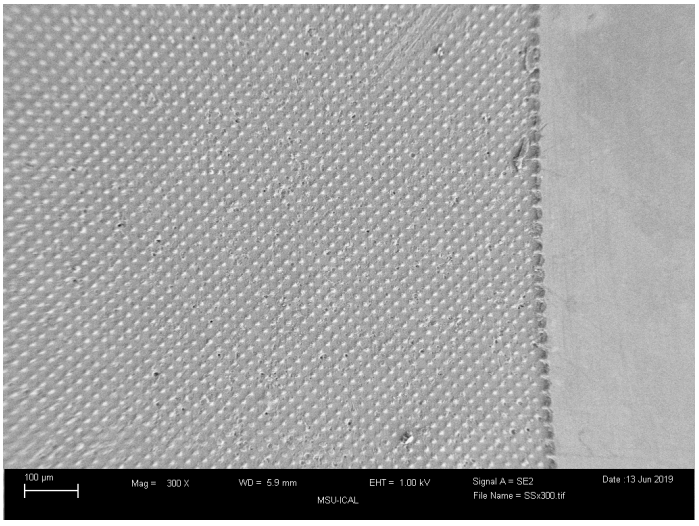


$10\times5\mu m$ Circular Single Spaced Pillars



$10\times5\mu m$ Circular Single Spaced Holes

$10\times5\mu m$ Square Double Spaced Pillars	
$10\times5\mu m$ Square Double Spaced Holes	

$10\times5\mu m$ Square Single Spaced Pillars	
$10\times5\mu m$ Square Single Spaced Holes	

APPENDIX B

CELL MASK FOR PHOTOLITHOGRAPHY

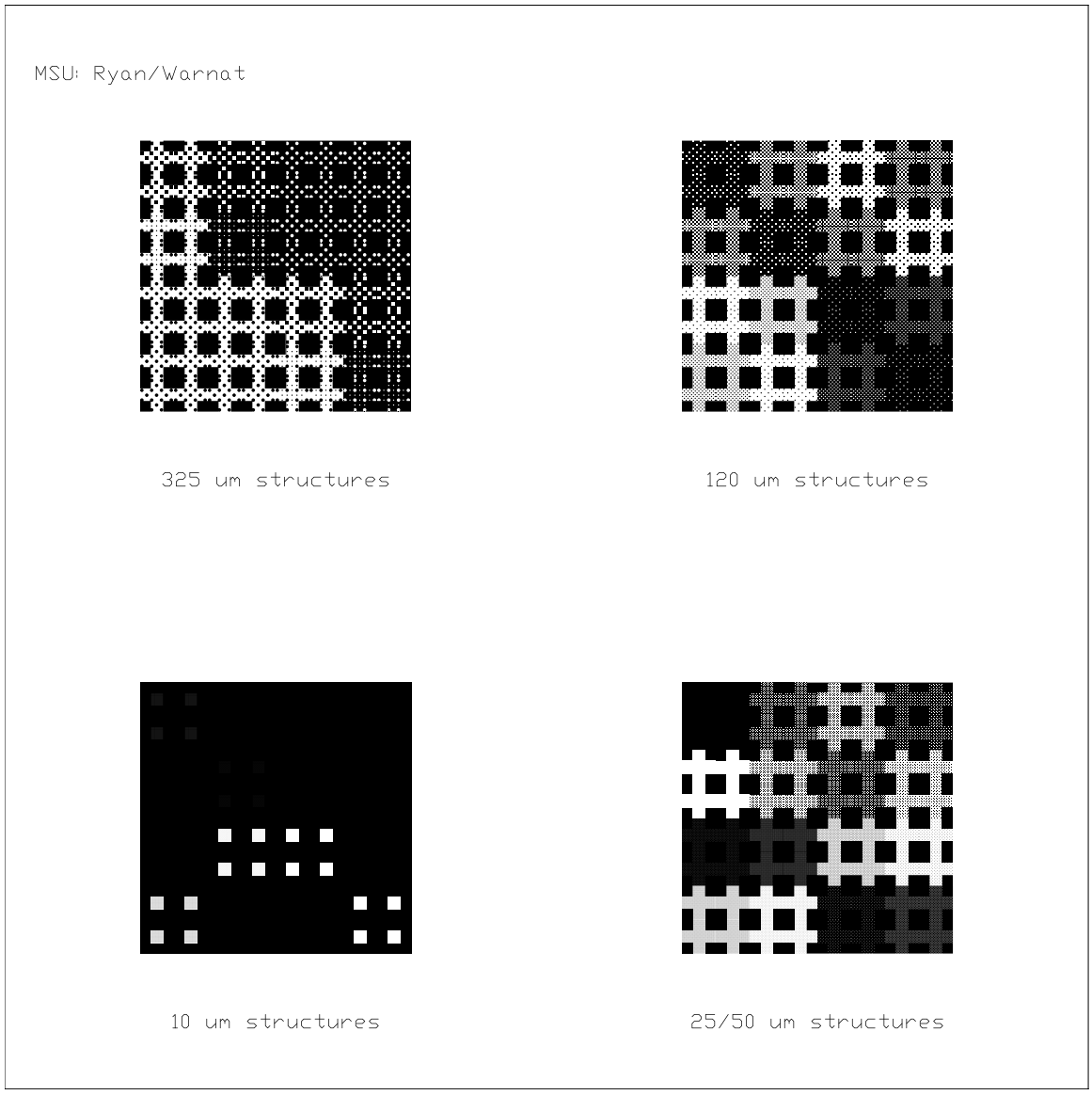


Figure B.1: Total Cell Mask

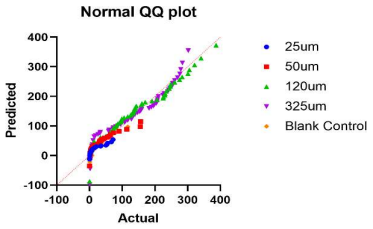
APPENDIX C

RESULTS OF GENERALIZED LINEAR MODEL

Analysis of variance (ANOVA) was used to analyze the data for statistically significant differences between cell counts when comparisons were isolated to the five different texture features. Most of the data followed a normal distribution, especially for feature size, however the data was not exactly normal and the results from ANOVA may have some weaknesses due to that. The consistently least normal data was the percentage of dead cells in the total number of cells for each sample. Bonferroni post testing was done to analyze which pillars had significant differences to the untextured control sample with the 120 and 325 μm features being the only features to significantly change from the control. All samples had percentages of dead cells to live cells that were statistically similar to that of the control sample. This indicates that cell viability was not significantly changed regardless of surface textures

Cell Counts by Size

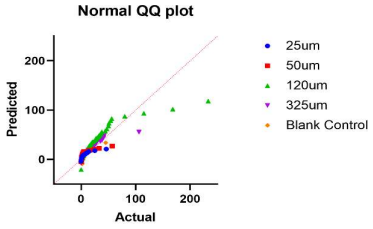
Live Cells



ANOVA summary	
F	26.26
P value	<0.0001
P value summary	****
Significant diff. among means (P < 0.05)?	Yes
R square	0.2967

Bonferroni's multiple comparisons test	**Mean Diff.**	**95.00% CI of diff.**	**Significant?**	**Summary**	**Adjusted P Value**	**E-?**	
Blank Control vs. 25um	27.07	-39.12 to 93.26	No	ns	>0.9999	A	25um
Blank Control vs. 50um	11.5	-55.70 to 78.69	No	ns	>0.9999	B	50um
Blank Control vs. 120um	-82.67	-148.1 to -17.26	Yes	**	0.0066	C	120um
Blank Control vs. 325um	-77.35	-142.8 to -11.94	Yes	*	0.0129	D	325um

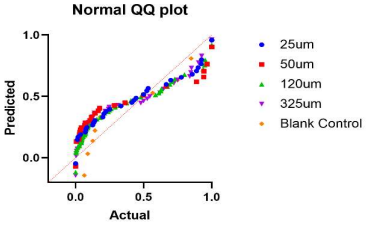
Dead Cells



ANOVA summary	
F	9.044
P value	<0.0001
P value summary	****
Significant diff. among means (P < 0.05)?	Yes
R square	0.1329

Bonferroni's multiple comparisons test	**Mean Diff.**	**95.00% CI of diff.**	**Significant?**	**Summary**	**Adjusted P Value**	**E-?**	
Blank Control vs. 25um	8.876	-10.93 to 28.68	No	ns	>0.9999	A	25um
Blank Control vs. 50um	8.475	-11.63 to 28.58	No	ns	>0.9999	B	50um
Blank Control vs. 120um	-12.6	-32.18 to 6.972	No	ns	0.4258	C	120um
Blank Control vs. 325um	-1.579	-21.44 to 18.28	No	ns	>0.9999	D	325um

Percentage of Dead Cells

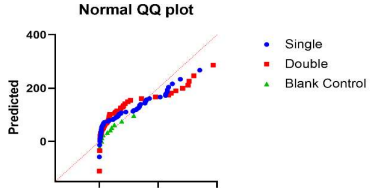


ANOVA summary	
F	1.233
P value	0.2975
P value summary	ns
Significant diff. among means (P < 0.05)?	No
R square	0.02127

Bonferroni's multiple comparisons test	**Mean Diff.**	**95.00% CI of diff.**	**Significant?**	**Summary**	**Adjusted P Value**	**E-?**	
Blank Control vs. 25um	-0.03475	-0.3286 to 0.2592	No	ns	>0.9999	A	25um
Blank Control vs. 50um	0.1054	-0.1922 to 0.4029	No	ns	>0.9999	B	50um
Blank Control vs. 120um	0.06491	-0.2231 to 0.3529	No	ns	>0.9999	C	120um
Blank Control vs. 325um	0.06536	-0.2268 to 0.3576	No	ns	>0.9999	D	325um

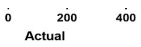
Cell Counts by Spacing

Live Cells



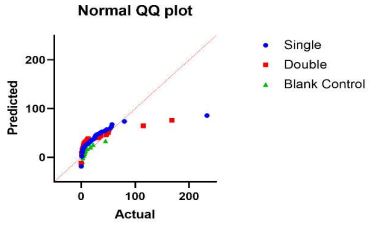
ANOVA summary	
F	0.3075
P value	0.7357
P value summary	ns
Significant diff. among means (P < 0.05)?	No

R square	0.003713



Bonferroni's multiple comparisons test	Mean Diff.	95.00% CI of diff.	Significant?	Summary	Adjusted P Value	C-?	
Blank Control vs. Single	-22.24	-86.51 to 42.02	No	ns	0.8695	A	Single
Blank Control vs. Double	-19.38	-84.38 to 45.62	No	ns	>0.9999	B	Double

Dead Cells

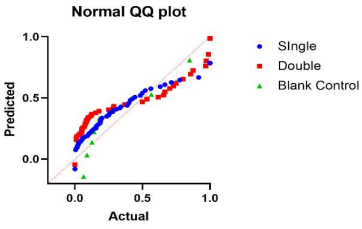


ANOVA summary

F	0.1399
P value	0.8695
P value summary	ns
Significant diff. among means (P < 0.05)?	No
R square	0.001693

Bonferroni's multiple comparisons test	Mean Diff.	95.00% CI of diff.	Significant?	Summary	Adjusted P Value	C-?	
Blank Control vs. Single	-0.446	-21.01 to 20.11	No	ns	>0.9999	A	Single
Blank Control vs. Double	1.839	-18.96 to 22.64	No	ns	>0.9999	B	Double

Percentage of Dead cells



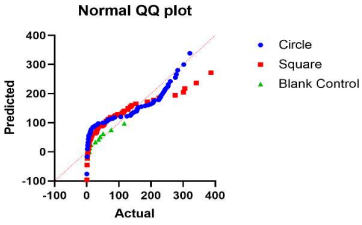
ANOVA summary

F	0.3461
P value	0.708
P value summary	ns
Significant diff. among means (P < 0.05)?	No
R square	0.004177

Bonferroni's multiple comparisons test	Mean Diff.	95.00% CI of diff.	Significant?	Summary	Adjusted P Value	C-?	
Blank Control vs. SIngle	0.08111	-0.1599 to 0.3221	No	ns	0.8951	A	SIngle
Blank Control vs. Double	0.08945	-0.1543 to 0.3332	No	ns	0.8153	B	Double

Cell Counts by Shape

Live Cells

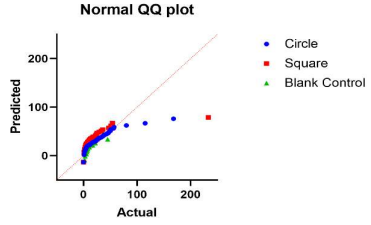


ANOVA summary

F	2.044
P value	0.132
P value summary	ns
Significant diff. among means (P < 0.05)?	No
R square	0.01866

Bonferroni's multiple comparisons test	Mean Diff.	95.00% CI of diff.	Significant?	Summary	Adjusted P Value	C-?	
Blank Control vs. Circle	-41.23	-109.0 to 26.56	No	ns	0.3424	A	Circle
Blank Control vs. Square	-19.23	-88.35 to 49.89	No	ns	>0.9999	B	Square

Dead Cells



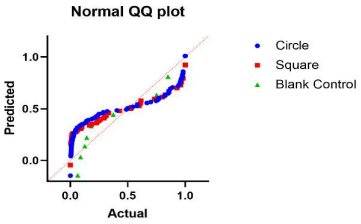
ANOVA summary

F	0.9346
P value	0.3943
P value summary	ns
Significant diff. among means (P < 0.05)?	No
R square	0.008619

Bonferroni's multiple comparisons test	Mean Diff.	95.00% CI of diff.	Significant?	Summary	Adjusted P Value	C-?

Blank Control vs. Circle	-1.71	-20.05 to 16.63	No	ns	>0.9999	A	Circle
Blank Control vs. Square	3.088	-15.61 to 21.79	No	ns	>0.9999	B	Square

Percentage of Dead Cells



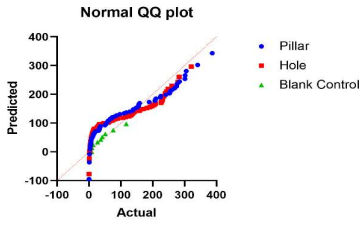
ANOVA summary

F	1.358
P value	0.2595
P value summary	ns
Significant diff. among means (P < 0.05)?	No
R square	0.01277

Bonferroni's multiple comparisons test	**Mean Diff.**	**95.00% CI of diff.**	**Significant?**	**Summary**	**Adjusted P Value**	**C-?**	
Blank Control vs. Circle	-0.001206	-0.2793 to 0.2769	No	ns	>0.9999	A	Circle
Blank Control vs. Square	0.08622	-0.1974 to 0.3699	No	ns	0.9866	B	Square

Cell Counts by Concavity/Convexity

Live Cells

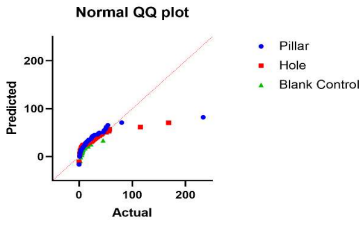


ANOVA summary

F	1.625
P value	0.1993
P value summary	ns
Significant diff. among means (P < 0.05)?	No
R square	0.01489

Bonferroni's multiple comparisons test	**Mean Diff.**	**95.00% CI of diff.**	**Significant?**	**Summary**	**Adjusted P Value**	**C-?**	
Blank Control vs. Pillar	-44.36	-114.3 to 25.59	No	ns	0.3075	A	Pillar
Blank Control vs. Hole	-26.46	-96.17 to 43.26	No	ns	0.7852	B	Hole

Dead Cells

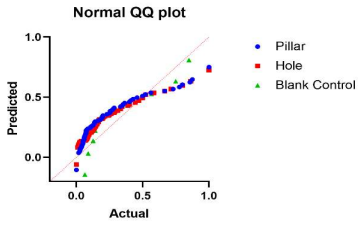


ANOVA summary

F	0.1002
P value	0.9047
P value summary	ns
Significant diff. among means (P < 0.05)?	No
R square	0.0009316

Bonferroni's multiple comparisons test	**Mean Diff.**	**95.00% CI of diff.**	**Significant?**	**Summary**	**Adjusted P Value**	**C-?**	
Blank Control vs. Pillar	-0.08	-18.44 to 18.28	No	ns	>0.9999	A	Pillar
Blank Control vs. Hole	1.415	-16.89 to 19.72	No	ns	>0.9999	B	Hole

Percentage of Dead Cells



ANOVA summary

F	1.318
P value	0.2699
P value summary	ns
Significant diff. among means (P < 0.05)?	No
R square	0.01222

Bonferroni's multiple comparisons test	**Mean Diff.**	**95.00% CI of diff.**	**Significant?**	**Summary**	**Adjusted P Value**	**C-?**	
Blank Control vs. Pillar	0.13	-0.07165 to 0.3317	No	ns	0.294	A	Pillar
Blank Control vs. Hole	0.1445	-0.05654 to 0.3455	No	ns	0.2124	B	Hole

APPENDIX D

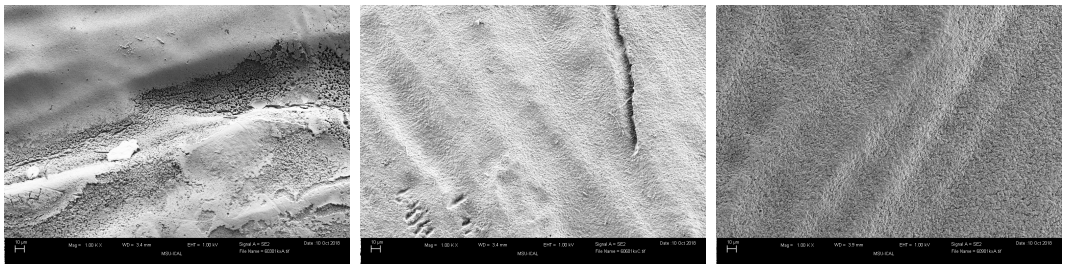
PIRANHA ETCH EXPERIMENTS

Methods

When the project began, different methods of modifying surface texture had to be explored. Acid etching was chosen as the first surface texturing method due to the availability of materials and the quick production turn around. The ability to make many samples quickly meant that procedures could be updated and experimented with quickly. Due to the chemical inertness of PEEK, very few solvents can erode the material. Sulfuric acid will have an effect over time, and piranha solution, a mixture of sulfuric acid and hydrogen peroxide, can be used to accelerate the corrosion. The mixture used in this experiment was a 3:1 mixture of 96% sulfuric acid to 30% hydrogen peroxide. It was heated to 60°C in order to accelerate the reaction, and the PEEK samples were submerged once the reaction reached 100°C. After 60 seconds of the sample being submerged, it would be removed and rinsed in DI water and sterilized through an acetone rinse and autoclaving. This method was experimented with 6mm thick sections of the 12.7mm diameter rods and 12.7mm diameter samples from the $80\mu m$ thick film. A regular, uniform surface texture could be achieved for the thicker disks at 60s of etching but was less reliable at other times. It is also important to note that no piranha etch method ever returned acceptable results on PEEK films. At lower etch times, films would have either an un-etched or highly irregularly etched surface. For longer periods of time, the samples would begin to rapidly dissolve. The rate at which the films would dissolved seemed to vary on a number of difficult to predict factors making identifying an ideal extraction time difficult. If this part of the experiment had continued, other methods of applying the solution other than submersion might have proven effective for PEEK films.

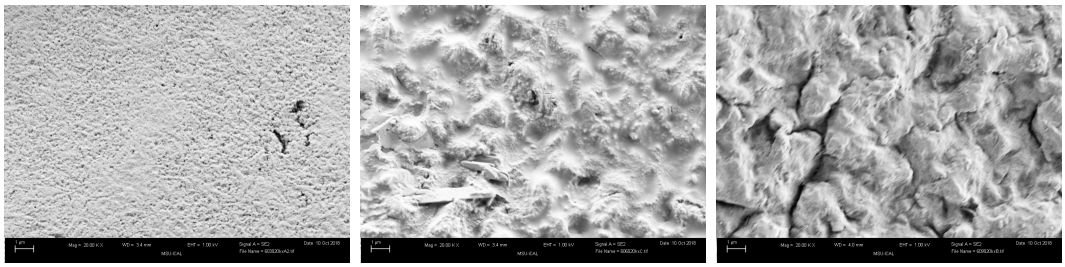
Results

Etch parameters and methods went through a great deal of development in order to get regular, uniform results. Even then the patterns were only uniform when compared to other etched PEEK samples and did not compare favorably with hot embossed textures. The regularity of the texture was measured through the dispersion of the texture width. Uniformity was a visual observation of regions on the sample that are textured similarly compared to the area of the whole sample. Initial results had irregular textures that would appear as strips of textured regions broken by untouched polymer. Heating the piranha solution at 60°C allowed the reaction to reach 100°C in a predictable manner. At this point the reaction was most capable of overcoming the chemical stability of PEEK and etching the surface.Different times were experimented with and 60 seconds of etchant exposure was determined to be the optimal exposure time. Less time would only etch the folds and imperfections in the bulk material such as in Figure D.1a, while etching too long would revert the PEEK to a smoother surface such as in Figure D.1c. This smoothing occurred when the etch would erode the features with the greatest surface area, etching for 60 seconds was determined to be the optimum time for preservation of the surface features first made by the etch as seen in Figure D.1b



(a) 30second Piranha etch (b) 60second Piranha etch (c) 90s Piranha etch

Figure D.1: Resultant Surface Textures on PEEK from Piranha Etch. Mag×1000

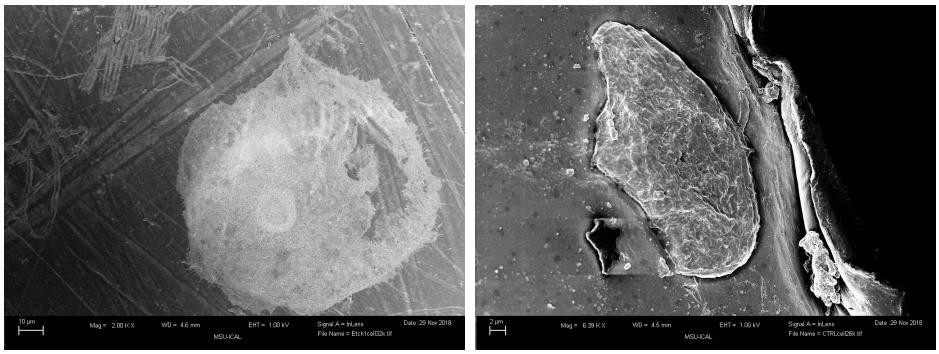


(a) 30s Piranha etch 20,000× (b) 60s Piranha etch 20,000× (c) 90s Piranha etch 20,000×

Figure D.2: Resultant Surface Textures on PEEK from Piranha Etch. Mag×20,000

Figure D.2a shows the surface features of samples exposed for 30 seconds in regions of the sample that did get etched. The small features are highly regular on the sub-micron level. This feature would have been desired to test against larger features but it's occurrence was irregular and it was impossible to texture an entire feature with it. Etching for 90 seconds would result in the features seen in Figure D.2c, larger micron sized features but irregularly shaped and spaced. The surface features seen in Figure D.2b resulted from 60 seconds of exposure and were determined to be the most regular and useful for growing cells on. The resultant cell growth was sparse for both the acid etched and the control samples. Very few cells could be observed under SEM on etched samples, and the cells that were imaged were heavily damaged during SEM, likely because of the vacuum. As a result, very few cells could be found on the samples and they were generally smaller than what was observed later in the project and in literature.

The effects of the different length scales in surface textures were brought into question here, laying the foundation for the research objectives. Samples etched at 30 seconds and 90 seconds were determined to be too irregular in their resultant etchings to warrant cell plating. The 60s etched samples were more regular than the others but



(a) Cell on Etched PEEK (b) 60s Piranha etch 20,000×

Figure D.3: Due to both the poor SEM fixing technique used and the poor cell attachment for these samples, the cells shown are small and damaged. The cell on the etched sample exhibited good adhesion but was damaged, likely due to the vacuum damaging the cell membrane D.3a. The control cell is small and located on the edge of the sample D.3b. Most cells on the control sample were heavily damaged.

still had inconsistencies within the sample. It was decided that greater control over surface texture was required, so many different surface texture characteristic could be modified and compared simultaneously.